

1 **Low Florida coral calcification rates in the Plio-Pleistocene**

2

3

4

5 **T.C. Brachert<sup>1,\*</sup>, M. Reuter<sup>2</sup>, S. Krüger<sup>1</sup>, J. S. Klaus<sup>3</sup>, K. Helmle<sup>4</sup> and J. M.**

6 **Lough<sup>5</sup>**

7

8

9 [1] {Institut für Geophysik und Geologie, Universität Leipzig, Leipzig, Germany }

10 [2] {Institut für Erdwissenschaften, Karl-Franzens-Universität Graz, Graz, Austria }

11 [3] {Department of Geological Sciences, University of Miami, Coral Gables, USA }

12 [4] {Oceanographic Center, Nova Southeastern University, Fort Lauderdale, USA }

13 [5] {Australian Institute of Marine Science, Townsville MC, Australia }

14

15

16 Correspondence to T. C. Brachert (brachert@uni-leipzig.de)

17

18

## 1 **Abstract**

2 In geological outcrops and drill cores from reef frameworks, the skeletons of scleractinian  
3 corals are usually leached and more or less completely transformed into sparry calcite because  
4 the highly porous skeletons formed of metastable aragonite ( $\text{CaCO}_3$ ) undergo rapid diagenetic  
5 alteration. Upon alteration, ghost structures of the distinct annual growth bands allow often  
6 for reconstructions of annual extension (= growth) rates, but information on skeletal density  
7 needed for reconstructions of calcification rates is invariably lost upon alteration. This report  
8 presents the first data of bulk density and calcification rates of fossil reef corals which  
9 escaped diagenetic alteration. The corals derive from unlithified shallow water carbonates of  
10 the Florida platform (southeastern USA), which formed during four interglacial sea level  
11 highstands dated 3.2, 2.9, 1.8, and 1.2 Ma in the mid Pliocene to early Pleistocene. With  
12 regard to the preservation, the coral skeletons display smooth growth surfaces with minor  
13 volumes of marine aragonite cement within intra-skeletal porosity. Within the skeletal  
14 structures, dissolution is minor along centers of calcification but lacks secondary cements.  
15 Mean extension rates were  $0.44 \pm 0.19 \text{ cm yr}^{-1}$  (range 0.16 to  $0.86 \text{ cm yr}^{-1}$ ), mean bulk density  
16 was  $0.96 \pm 0.36 \text{ g cm}^{-3}$  (range 0.55 to  $1.83 \text{ g cm}^{-3}$ ) and calcification rates ranged from 0.18 to  
17  $0.82 \text{ g cm}^{-2} \text{ yr}^{-1}$  (mean  $0.38 \pm 0.16 \text{ g cm}^{-2} \text{ yr}^{-1}$ ), values which are 50 % of modern shallow-  
18 water reef corals. To understand the possible mechanisms behind these low calcification rates,  
19 we compared the fossil calcification rates with those of modern zooxanthellate-corals (z-  
20 coral) from the Western Atlantic (WA) and Indo-Pacific calibrated against sea surface  
21 temperature (SST). In the fossil data, we found a widely analogous relationship with SST in z-  
22 corals from the WA, i.e. density increases and extension rate decreases with increasing SST,  
23 but over a significantly larger temperature window during the Plio-Pleistocene. With regard to  
24 the environment of coral growth, stable isotope proxy data from the fossil corals and the  
25 overall structure of the ancient shallow marine communities are consistent with a well-mixed,  
26 open marine environment similar to the present-day Florida Reef Tract (FRT), but variably

1 affected by intermittent upwelling. Upwelling along the platform may explain low rates of  
2 reef coral calcification and inorganic cementation, but is too localized to account also for low  
3 extension rates of Pliocene z-corals throughout the tropical Caribbean in the western Atlantic  
4 region. Low aragonite saturation on a more global scale in response to rapid  
5 glacial/interglacial CO<sub>2</sub> cyclicity is also a potential factor, but Plio-Pleistocene atmospheric  
6 *p*CO<sub>2</sub> is believed to have been broadly similar to the present-day. Heat stress related to  
7 globally high interglacial SST only episodically moderated by intermittent upwelling  
8 affecting the Florida platform seems to be another likely reason for low calcification rates.  
9 From these observations we suggest some present coral reef systems to be endangered from  
10 future ocean warming.

11

## 12 **1 Introduction**

### 13 **1.1 Architecture of the zooxanthellate coral skeleton and systematics of** 14 **skeletal calcification**

15 The skeleton of zooxanthellate corals (z-corals) is a highly organized, porous hard tissue  
16 formed of mineral CaCO<sub>3</sub> (aragonite). In X-ray images of slices parallel to the axes of the  
17 corallites (axes of maximum growth), massive z-coral skeletons typically display alternations  
18 of light and dark bands. One pair of these “density bands” typically represents one year of  
19 growth (Knutson et al., 1972) and forms the basis for the calibration of internal age models  
20 and for estimates of the extension rates, i.e. the rate of upward and outward growth of the  
21 colony surface (Lough and Cooper, 2011). Skeletal bulk density is a measure of the volume of  
22 pore volumes within the skeleton; the less porosity the closer will be the density to that of  
23 mineral aragonite (2.93 g cm<sup>-3</sup>). Extension rate and density combine for estimates of  
24 calcification rates according to equation (1) (Lough and Cooper, 2011):

25

1 calcification rate ( $\text{g cm}^{-2} \text{ yr}^{-1}$ ) = annual extension rate ( $\text{cm yr}^{-1}$ ) x density ( $\text{g cm}^{-3}$ ) (1)In  
2 addition to the basic calcification parameters described above, serial chemical and isotope  
3 proxy data retrieved along the direction of maximum skeletal extension provide independent  
4 quantitative measures of the environment. Stable isotope ratios of the oxygen ( $\delta^{18}\text{O}$ ) are  
5 sensitive to sea surface water temperature (SST) and serial samples over the growth bands  
6 allow for the documentation of seasonal or interannual SST variability on multi-annual time-  
7 scales (decade and century scale) (Felis and Pätzold, 2004; Leder et al., 1996; Swart, 1983).  
8 Limitations of the method pertain to the influence of seawater  $\delta^{18}\text{O}$  which is subject to  
9 changes due to precipitation/evaporation (i.e. salinity) and river discharge. To overcome the  
10 problem of seawater  $\delta^{18}\text{O}$  for making estimates of salinity excursions from normal seawater,  
11 chemical element proxies of SST rather insensitive to salinity are in use (Sr/Ca, U/Ca, Mg/Ca)  
12 in combination with skeletal  $\delta^{18}\text{O}$  (Felis et al., 2004; Shen and Dunbar, 1995; Swart, 1981).  
13 Other chemical elements and carbon stable isotope ratios have been shown to be recording  
14 sensitively productivity, river discharge, pH, or also subtle diagenetic alterations (Ba/Ca,  
15 Y/Ca, B/Ca,  $\delta^{13}\text{C}$ ) (Allison et al., 2007; McCulloch et al., 2003; Sinclair et al., 1998; Swart et  
16 al., 2010).  
17 In the geological record, the skeletons of scleractinian corals and other sedimentary grains  
18 composed originally of metastable aragonite ( $\text{CaCO}_3$ ) usually form moldic porosity, or are  
19 more or less completely replaced by mosaics of blocky calcite spar (Schroeder and Purser,  
20 1986). Although these secondary alterations generally pose no problem for classical  
21 approaches in paleoecology and taxonomy, all information stored as isotope and geochemical  
22 proxy data has been reset and makes the corals no longer available as environmental or  
23 geochronological archives. The first diagenetic alterations of the skeletons still happen at the  
24 sea floor, in deeper parts of the skeleton where the living organic tissues were previously  
25 withdrawn. These alterations represent growths of inorganic aragonite fiber crystals and  
26 subtle dissolution phenomena within the centers of calcification (COC) (Perrin, 2004).

1 Differential diagenetic processes on crystalline phases and organic matrices also exist and  
2 include aragonite – aragonite recrystallizations associated with a loss of micron-sized growth  
3 information (McGregor and Gagan, 2003; Nothdurft and Webb, 2009; Perrin, 2004). In  
4 contrast, in the classical freshwater diagenetic environment, the primary surface area of the  
5 skeleton controls diagenetic susceptibility and rates of alteration (Constantz, 1986; Dullo,  
6 1984). The freshwater effects are dominated by dissolution via moldic porosity and  
7 subsequent reduction of pore spaces by cementation, or dissolution and associated  
8 crystallization of blocky calcite without developing a significant moldic stage (Bathurst,  
9 1975). In the latter process, ghost structures reflecting original microstructures will be  
10 preserved (Flügel, 2004). More often, ghost structures of the growth bands form by subtle,  
11 diffusion-controlled dissolution which preferentially starts at the COCs and continues to form  
12 increasingly hollow skeletal structures (Reuter et al., 2005). The rate of skeleton-internal  
13 dissolution via diffusion differs among growth bands within a specimen and responds to  
14 bands of higher and lower density (Reuter et al., 2005). Given the situation where no  
15 secondary addition of carbonate material has taken place, however, the hollow structures may  
16 still be suitable for isotope and geochemical proxy analysis (Mertz-Kraus et al., 2009a; Mertz-  
17 Kraus et al., 2008; Mertz-Kraus et al., 2009b). Following infilling by late diagenetic calcite  
18 spar, this differential dissolution process leaves records of growth bands from which skeletal  
19 extension (= colony growth per year) can be retrieved (Brachert et al., 2006b; Johnson and  
20 Pérez, 2006; Shinn, 1966). But, this process of dissolution and subsequent cementation of  
21 moldic and intra-particle porosity tends to destroy all information pertaining to skeletal  
22 density. Alteration of the primary skeleton along this diagenetic pathway is obvious by the  
23 presence of calcite, either replacing skeletal structures or infilling skeletal porosity. While the  
24 petrographic aspect of the calcite documents the type of freshwater or burial alteration  
25 environment, cathodoluminescence analysis and geochemical data may provide further  
26 information as to the redox character of the diagenetic fluids (Flügel, 2004). Alteration of

1 aragonite is commonly a rapid process, but in the rare event of low pore-water circulation  
2 rates, corals do escape diagenetic alteration (Anagnostou et al., 2011; Brachert et al., 2006a;  
3 Brachert et al., 2016; Denniston et al., 2008a; Gothmann et al., 2015; Griffiths et al.,  
4 2013){Mertz-Kraus, 2008 #15146}.

5         In this study we present calcification data from extremely well preserved z-corals with  
6 intact skeletal density from Plio-Pleistocene interglacial deposits on the Florida platform  
7 (USA; Fig. 1). We show that calcification rates were 50 % lower than they are in the present-  
8 day Western Atlantic (WA). For an understanding of the possible mechanisms behind these  
9 low calcification rates, we use modern analogue data compiled from the literature on recent z-  
10 corals of the WA and Indo-Pacific (IP). According to this database, temperature generally  
11 boosts calcification rates in modern z-corals, but field studies on single species of z-coral  
12 suggest the rates to decline beyond optimum values (Carricart-Ganivet et al., 2012; Cooper et  
13 al., 2008). The non-linearity of calcification rates ( $\text{g cm}^{-2} \text{ yr}^{-1}$ ) derives from inputs of two  
14 independent variables: skeletal growth rate (extension rate,  $\text{cm yr}^{-1}$ ) and skeletal density ( $\text{g}$   
15  $\text{cm}^{-3}$ ) (Lough, 2008). The temperature effects on extension rates of *Porites* from the IP are  
16 well documented over a large temperature window and display slow increases with  
17 temperature below but sharp decreases above optimum (Cantin et al., 2010; Carricart-Ganivet  
18 et al., 2012; Lough and Barnes, 2000). The temperature responses of extension rate and  
19 density, however, are generally believed to markedly differ according to taxon and/or ocean  
20 region (Highsmith, 1979) and are further complicated by proximity trends reflecting  
21 temperature and seasonality gradients, exposure, efluxes of “inimical” bank waters, or  
22 nutrient supplies (Lough and Cooper, 2011; Manzello et al., 2015b). We discuss whether the  
23 patterns of z-coral calcification found in the fossils from the Florida Platform is a local or  
24 global signature corresponding with temperature stress or low supersaturation of the sea  
25 water with respect to aragonite ( $\Omega_{\text{aragonite}}$ ) during the Plio-Pleistocene interglacials. This study  
26 complements two previous studies using sclerochronology of bivalves and z-corals for

1 reconstructions of the paleoenvironments and long-term changes of seasonality in southern  
2 Florida (Brachert et al., 2016; Brachert et al., 2014).

3

#### 4 **1.2 The Florida Platform during the Plio-Pleistocene interglacials**

5 During the Plio-Pleistocene interglacials, global sea levels were up to 22 m (Miller et al.,  
6 2012) or even 35 m higher (Dowsett and Cronin, 1990) and global mean temperatures 2 to  
7 4°C warmer than present, whereas SSTs of the warm pools at low latitudes were ~2°C higher  
8 than present (Fedorov et al., 2013; O'Brien et al., 2014). Although dramatic cooling occurred  
9 in the high latitudes, long-term atmospheric  $p\text{CO}_2$  appears to have remained rather constant  
10 after the mid Pliocene climatic optimum (~3 Ma) until the present (Seki et al., 2010). During  
11 and before the optimum, however,  $p\text{CO}_2$  reached values expected for the end of this century  
12 through the burning of fossil fuels (IPCC, 2013; Seki et al., 2010). Modeling of the oceanic  
13 carbonate systems suggest the long-term  $p\text{CO}_2$  changes to have had no effect on the saturation  
14 state of seawater with regard to  $\Omega_{\text{aragonite}}$  (Hönisch et al., 2012), but evidence exists that rates  
15 of carbonate precipitation and skeletal accretion of planktic foraminifera differed over the last  
16 glacial / interglacial cycle, in response to changes of  $\Omega_{\text{aragonite}}$  driven by  $p\text{CO}_2$  (Barker, 1986;  
17 Beaufort et al., 2011; Riding et al., 2014).

18

19 The Plio-Pleistocene Florida carbonate platform represents a stack of shallow marine  
20 carbonate sequences formed during sea level highstands which are separated by paleosols or  
21 thin freshwater units formed during lowstands. A pronounced reef system existed along the  
22 southwestern margin of the peninsula (Meeder, 1979). The single unlithified, marine units  
23 contain a diverse mollusk and coral fauna comparable to that of the present reef tracts and  
24 back-reef systems (Meeder, 1979; Petuch and Roberts, 2007). Combined oxygen and carbon  
25 stable isotope data ( $\delta^{18}\text{O}$ ,  $\delta^{13}\text{C}$ ) of diagenetically pristine mollusks and z-corals from the  
26 platform sediments reflect the complexity of the depositional setting including brackish to

1 hypersaline and well-mixed, open marine environments (Brachert et al., 2014; Lloyd, 1969;  
2 Tao and Grossman, 2010). The reasons for high benthic carbonate productivity by mollusks  
3 during the Plio-Pleistocene is controversial, and has been suggested to be due to high nutrient  
4 concentrations resulting from freshwater input (Tao and Grossman, 2010) or upwelling  
5 (Allmon, 2001; Allmon et al., 1995; Brachert et al., 2016; Emslie and Morgan, 1994; Jones  
6 and Allmon, 1995). Recently, SST estimates for the Pliocene and Pleistocene interglacial  
7 units based on  $\delta^{18}\text{O}$  values retrieved from the reef coral *Orbicella* and assuming a modern  
8 seawater value for  $\delta^{18}\text{O}$  ( $\delta^{18}\text{O}_{\text{water}}$ ) at the Florida Reef Tract (FRT) (Leder et al., 1996) yielded  
9 mean annual SSTs between 19.5 and 26.0 °C; the lowest temperatures occurred during  
10 episodes of maximum upwelling according to their  $\delta^{13}\text{C}$  values (Brachert et al., 2016). Apart  
11 from low SSTs believed to be essentially the effect of upwelling, the large range of values is  
12 likely in part an artifact of the uniform value for seawater  $\delta^{18}\text{O}$  ( $\delta^{18}\text{O}_{\text{water}}$ ) used for the  
13 calculations, irrespective of sampling locality and stratigraphic unit (Brachert et al., 2016). In  
14 contrast, seasonal SST variability (~7 °C) inferred from cyclic  $\delta^{18}\text{O}$  variations of the fossils is  
15 independent of assumptions of  $\delta^{18}\text{O}_{\text{water}}$ . Reconstructed seasonality is not only remarkably  
16 constant within specimens and over the last 3.2 Ma, but also fits modern surface seasonality  
17 along the reef tract (Brachert et al., 2016; Brachert et al., 2014). Large seasonality as  
18 prevailing off North Carolina (Macintyre and Pilkey, 1969) or in inner coastal waters of  
19 Florida Bay (FB) (Swart et al., 1996) has not been encountered in the data from the reef corals  
20 and has also been taken for inferring a normal shallow-marine environment without unusual  
21 stress from cool waters or evaporation and freshwater influxes (Brachert et al., 2014).

22

23 In southern Florida, the most extensive growth of reef corals occurs at present along the FRT  
24 on the Atlantic side of the peninsula, whereas only limited z-coral growth occurs along the  
25 Gulf side in the west and the shallow FB in the southeast. On the Atlantic side, coral



1 communities are characterized by diverse stands comprising abundant *Orbicella* (Lidz, 2011),  
2 whereas on the Gulf side and in FB, coral growth is restricted to the two eurytopic taxa  
3 *Siderastrea* and *Solenastrea* (Okazaki et al., 2013; Swart et al., 1999). Published extension  
4 rates for recent *Solenastrea* inhabiting the most marine segments of FB range from 0.51 to 0.9  
5 cm yr<sup>-1</sup> (Hudson et al., 1989; Swart et al., 1996). Recent *Solenastrea* has also been recorded to  
6 grow under rather cold water conditions along the US southeastern Atlantic coast off North  
7 Carolina (Macintyre and Pilkey, 1969), but quantitative calcification data from that setting are  
8 not available, leaving the question unanswered regarding the effects of low SST on extension  
9 and density. Colony sizes at the northern sites similar to those of the lower latitudes have been  
10 suggested to indicate similar extension and calcification rates, however (Macintyre and  
11 Pilkey, 1969).

12

13

14

### 15 **1.3 Materials**

16 Z-corals were sampled from four distinct stratigraphic units of the Florida carbonate platform  
17 (USA) representing interglacial highstands of sea level subsequent to the Pliocene warm  
18 period, dated 3.2, 2.9, 1.8 and 1.2 million years (Ma) of the mid Pliocene and early  
19 Pleistocene (Fig. 1, Tab. 1) (Brachert et al., 2014). Our own sampling focused on *Solenastrea*  
20 ( $n = 11$ ) which is a common taxon in the Plio-Pleistocene shallow water carbonates of  
21 southwestern Florida. This dataset was complemented by specimens of *Orbicella* ( $n = 2$ ) and  
22 *Porites* ( $n = 1$ ) and one dataset of a *Solenastrea* taken from the literature comprising serial  
23  $\delta^{18}\text{O}$  and  $\delta^{13}\text{C}$  values and annual extension rates (Roulier and Quinn, 1995) (Tab. 1).

24

### 25 **1.4 Methods**

1 Fossil corals selected for this study were cut into <1cm thick slabs along the plane of  
2 maximum growth using a conventional rock saw equipped with a water-cooled diamond  
3 blade. All corals were screened for diagenetic alteration using a binocular microscope and  
4 scanning electron microscope (SEM). In order to detect minimal contaminations by secondary  
5 calcite, powder samples taken at random were prepared for X-ray diffraction (XRD) and  
6 analysed using a Rigaku Miniflex diffractometer at angles between 20° to 60° 2θ. Only  
7 skeletal areas that retained their original aragonite mineralogy (XRD), skeletal porosity and  
8 microstructure without evidence for significant secondary crystal growth or dissolution  
9 (microscopic and SEM observation) were accepted for further sample preparation. Coral slabs  
10 of equal thickness were X-rayed using a digital X-ray cabinet (SHR 50 V) to identify potential  
11 zones of diagenetic alteration (McGregor and Gagan, 2003; Reuter et al., 2005), bioerosion,  
12 and to document the density bands (Knutson et al., 1972). One coral specimen (452K1) was  
13 analysed geochemically using LA-ICP-MS (Böcker, 2014) with regard to concentrations of  
14 environmentally sensitive elements (e.g. Sr/Ca, U/Ca, B/Ca) and following recommendations  
15 for evaluating the diagenetic status of corals from strongly lithified and altered limestone  
16 (Anagnostou et al., 2011; Gothmann et al., 2015). LA-ICP-MS analyses were performed at  
17 the Max Planck-Institut für Chemie (Mainz, Germany) using a NewWave UP 213 laser  
18 ablation system coupled to a ThermoFisher Element 2 ICP-MS with a Nd:YAG laser. Laser  
19 spots were aligned along transects and 0.5 mm apart with a laser spot size of 80 µm. Blanks  
20 (20 s) were measured prior to each measurement, dwell time was 70 s. For calibrations, the  
21 reference glass NIST 612 and synthetic carbonate USGS MACS-1 (Jochum et al., 2011) was  
22 used and measured twice at the beginning, after 30 spots and at the ends of transects.  
23  
24 Quantitative density measurements were made using the software CoralXDS (freeware)  
25 according to Helmle and co-workers (Helmle et al., 2002). In this approach, the CoralXDS  
26 software compares the gray values recorded in X-radiographs from corals with those from

1 aluminum plates having the same thickness as a background picture and an aluminum wedge  
2 for density calculations. Measurements were done along transects parallel to the corallites and  
3 parallel to the sampling transects for stable isotope analyses (Brachert et al., 2016). Bulk  
4 skeletal density was calculated as the mean of all individual measurements taken along a  
5 given transect. Calibration of the measurements was tested by measurements of standards for  
6 zero density (air) and massive aragonite (slice of a *Glycimeris* bivalve shell having a thickness  
7 equaling that of the coral slice). External analytical precision of the routine measurements was  
8 tested by double blind measurements, and mean deviation from regression ( $R^2 = 0.91$ ,  $p <$   
9  $0.05$ ) was found to be  $0.04 \pm 0.01$  g cm<sup>-3</sup> (range = 0.02 to 0.05 g cm<sup>-3</sup>; n = 18).

10

11 As a baseline for the description and interpretation of the data from the fossils, we use  
12 calcification data from recent corals reported in the literature deriving equally from tropical  
13 and high latitudinal localities within the shallow-water reef belt (Baker and Weber, 1975;  
14 Bessat and Buigues, 2001; Carricart-Ganivet et al., 2000; Carricart-Ganivet and Merino,  
15 2001; Dodge and Brass, 1984; Dustan, 1975; Elizalde-Rendon et al., 2010; Fabricius et al.,  
16 2011; Goodkin et al., 2011; Graus and Macintyre, 1982; Helmle et al., 2011; Highsmith et al.,  
17 1983; Hudson et al., 1989; Lough, 2008; Mallela and Perry, 2007; Tanzil et al., 2009), and  
18 one unpublished record of *Solenastrea* from FB (FB-6). We present a set of three descriptive  
19 diagrams for a comparison of the patterns of calcification (extension rate, bulk density,  
20 calcification rate) in the modern and fossil z-corals on the basis of linear regression. For a  
21 deeper understanding of the processes, we further apply quadratic polynomial regression  
22 models of experimental data calibrated with SST to account for the established non-linearity  
23 of life processes.

24

25 Stable isotope data described here are the same as reported in companion publications by  
26 Brachert et al. (2014, 2016), and only a short summary of the methodology is given here.

1 Sample powders for stable isotope analysis were taken using a microdrill equipped with a 0.6  
2 mm drill bit. Prior to sampling of the corallite walls, all endothecal skeletal elements were  
3 removed. For stable isotope analysis, carbonate powders were reacted with 102% phosphoric  
4 acid at 70°C using a Kiel IV online carbonate preparation line connected to a MAT 253 mass  
5 spectrometer. All carbonate values are reported in per mil (‰) relative to PDB according to  
6 the delta notation. Reproducibility was checked by replicate analysis of laboratory standards  
7 and was better than  $\pm 0.06\text{‰}$  ( $1\sigma$ ) for oxygen isotopes ( $\delta^{18}\text{O}$ ).

8

9 The scleractinian genus name *Orbicella* is used for corals previously assigned to *Montastraea*  
10 according to the revised taxonomic classification of the reef coral family Mussidae by (Budd  
11 et al., 2012). According to the same work (op. cit.), the genus *Diploria* has been split into the  
12 genera *Diploria* and *Pseudodiploria*. We use the two genus names in combination as  
13 *Diploria/Pseudodiploria*, because our database likely incorporates material from both genera  
14 sensu Budd et al. (2012).

15

16 Statistical analyses were performed using the PAST paleontological statistics software  
17 package (version 3.01) for education and data analysis (freeware [folk.uio.no/ohammer/past/](http://folk.uio.no/ohammer/past/)).

18 Variability of stable isotope data ( $\delta^{18}\text{O}$ ,  $\delta^{13}\text{C}$ ) was evaluated using the T-test. A linear  
19 bivariate model was tested as to whether there were no statistical differences in the stable  
20 isotope values in a dataset ( $p > 0.05$ ) against the alternate hypothesis that there were  
21 significant differences ( $p < 0.05$ ). Equality of regression slopes was tested using the F-test as  
22 assumed by analyses of covariance (ANCOVA). One-way analysis of variance (ANOVA)  
23 tested if there were no statistical differences in the mean growth parameters (extension,  
24 density, calcification) between two given coral sites ( $p > 0.05$ ) against the alternate hypothesis  
25 that there were significant differences ( $p < 0.05$ ).

26

## 1    **2    Results and discussion**

### 2    **2.1    Preservation**

3    The metastable carbonate mineral aragonite forming the z-coral skeleton is prone to  
4    modification by leaching, cementation and mineral transformation causing skeletal density to  
5    be reduced or enhanced. Visual inspection of the skeletons using a binocular microscope (x 15  
6    enlargement) and SEM revealed clean skeletal surfaces not covered systematically by  
7    secondary cements, except for localized, micron-scaled patches of spherulitic aragonite or  
8    patches of isopachous aragonite (Böcker, 2014). SEM observation has not revealed any  
9    evidence for aragonite – aragonite recrystallizations (Fig. 2) but some porosity within the  
10    centers of calcification (COCs). The latter does indeed imply some dissolution has occurred,  
11    and therefore, subtle reductions of skeletal density (Fig. 2), however, since dissolution at the  
12    COCs has also been reported from recent specimens (Perrin, 2004), this effect may also be  
13    present in the data from recent corals.

14    Secondary calcite is not documented by XRD analysis (detection limit of the method ~1%)  
15    and has very rarely been observed to occur within skeletal growth porosity but never within  
16    voids formed by preferential dissolution of the COCs. Published geochemical screenings  
17    using LA-ICP-MS for specimen 452 K1 (Böcker, 2014) documented variable ratios of Sr/Ca  
18    and U/Ca which are in phase with serial  $\delta^{18}\text{O}$  data. These element ratios reflect SST variations  
19    consistent with reconstructions on the basis of serial  $\delta^{18}\text{O}$  values and recent instrumental  
20    seasonality along the FRT (Böcker, 2014). The positive correlation of the Sr/Ca with U/Ca  
21    and the B/Ca ratios fluctuating between 0.3 and 0.6 mmol/mol is fully consistent with modern  
22    z-corals and implies little alteration has taken place, especially because boron is known to be  
23    a diagenetically highly volatile element (Allison et al., 2010; Böcker, 2014). According to our  
24    conviction, all these data provide no critical evidence for the alteration of the original  
25    skeleton. Because of this line of reasoning and low overall calcite content evident from XRD  
26    analysis (calcite below detection limits), we refrained from measuring element ratios sensitive

1 to the redox conditions of calcite precipitating freshwaters or burial fluids (Fe/Ca, Mn/Ca) and  
2 other more sophisticated geochemical methods as potential measures of alteration  
3 (Anagnostou et al., 2011; Gothmann et al., 2015).  
4  
5 X-radiographs display very regular expressions of density bands, concordant with the growth  
6 structures of the skeleton and stable isotope records, but no cloudy density variations or  
7 patches of high (low) density as documented from diagenetically-altered specimens (Böcker,  
8 2014; Brachert et al., 2006a; Mertz-Kraus, 2009). The presence of concordant density bands  
9 implies the preservation of original density variations of the skeleton and, therefore, supports  
10 the conclusion of a pristine state of preservation for the specimens under consideration (Fig.  
11 3). In contrast to density, extension rate is not sensitive to diagenetic alterations and many  
12 data have been retrieved earlier from highly altered fossil coral specimens of the WA region  
13 (Brachert et al., 2006b; Gischler et al., 2009; Johnson and Pérez, 2006; Reuter et al., 2005). It  
14 should be noted that density was measured using X-ray densitometry along transects defined  
15 from visual inspection of radiographs, and measurements were taken only in segments of the  
16 skeleton not affected by borings (bivalves, sponges, sipunculids) or embedded encrusting  
17 biota (serpulids, bivalves). Bulk density data presented by this study and in a companion  
18 publication (Brachert et al., 2016), are therefore, not influenced by the volume of biogenic  
19 borings or incrustations, although these effects may also be inherent to published density data  
20 of recent corals. This is an important issue, because other approaches have used “net density”  
21 (i.e. the integrative weight of carbonate laid down by the coral and encrusting biota minus  
22 losses by bioerosion within a volume) for comparative calcification studies (see (Kuffner et  
23 al., 2013). In sum, all of these observations and reasoning suggest the z-corals selected for this  
24 calcifications study to be essentially unaltered by diagenesis and X-ray densitometry to  
25 produce robust data.

26

## 1   **2.2   Calcification**

2   The Pliocene and Pleistocene z-corals from the Florida Platform display extension rates that  
3   range from 0.16 to 0.86 cm yr<sup>-1</sup> with a mean value of  $0.44 \pm 0.19$  cm yr<sup>-1</sup> ( $n = 15$ ,  $\pm 1\sigma$ ), bulk  
4   skeletal densities between 0.55 and 1.52 g cm<sup>-3</sup> with a mean of  $0.86 \pm 0.22$  g cm<sup>-3</sup> ( $n = 14$ ),  
5   and skeletal calcification rates from 0.18 to 0.54 g cm<sup>-2</sup> yr<sup>-1</sup> with a mean =  $0.34 + 0.11$  g cm<sup>-2</sup>  
6   yr<sup>-1</sup> ( $n = 14$ ) (Fig. 4, Tab. 3). Annual extension rates and bulk skeletal density show a  
7   significant negative correlation ( $R^2 = 0.329$ ;  $p = 0.026$ ), i.e. density decreases with increasing  
8   extension rates. In contrast, extension rates and calcification rates display a positive  
9   relationship ( $R^2 = 0.484$ ;  $p = 0.004$ ), which implies that calcification rates also decline with  
10   increasing extension. Lastly, bulk density and calcification display no relationship ( $R^2 =$   
11    $0.025$ ;  $p = 0.797$ ) (Fig. 4). Although no statistics were applied to the data of *Orbicella* ( $n = 2$ )  
12   and *Porites* ( $n = 1$ ) their calcification systematics seem to be indistinguishable from those of  
13   *Solenastrea* according to visual assessment (Fig. 4). With regard to variability over geological  
14   time, extension rate, bulk density and calcification rate of the three genera *Solenastrea*,  
15   *Orbicella* and *Porites* from the Florida platform were plotted according to four time-slices  
16   3.2, 2.9, 1.8, and 1.2 Ma (Fig. 5, Tab. 1, 2), and all calcification data were found to be  
17   undistinguishable among time-slices according to ANOVA ( $p > 0.05$ ). Published extension  
18   rates of z-corals reported from various other fossil low-latitude sites of the Western Atlantic  
19   region are  $\sim 0.3$  cm yr<sup>-1</sup> in late Miocene reefs (Denniston et al., 2008b) and range from 0.3 to  
20   0.8 cm yr<sup>-1</sup> in Pliocene units (Johnson and Pérez, 2006), whereas they were 0.2 and 1.0 cm yr<sup>-1</sup>  
21   <sup>1</sup> in the FRT during the late Pleistocene (0.13 Ma) (Gischler et al., 2009). As such, they are all  
22   consistent with the low extension rates reported by our study (Fig. 4). Importantly, skeletal  
23   density data are not available from these sites due to pervasive diagenetic alterations, and  
24   therefore, skeletal density and calcification rates are not known, however.

25

1 For the recent time-slice (0 Ma) we use analogue data from southern Florida published in the  
2 literature and complemented in part by one new set of average values (FB-6) published here  
3 for the first time (Tab. 4).

4

5 The extension rates of recent *Solenastrea* from FB range from 0.51 to 0.89 cm yr<sup>-1</sup> and are  
6 fully within the range found in the Pliocene and Pleistocene corals (Fig. 5). Density values  
7 have not been published from FB z-corals so far; we measured a density of 1.07 g cm<sup>-3</sup> (Tab.  
8 2) which is compatible with fossil *Solenastrea*. The same is true for the *Orbicella* from FRT  
9 as compared to the two fossil *Orbicella*, whereas the density records available from the FRT-  
10 *Porites* are substantially above that from the fossil *Porites* which is near the lower end of the  
11 spectrum (Fig. 5, Tab. 4). Finally, calcification rates of all three taxa of the recent z-corals in  
12 FB and FRT tend to be above the Plio-Pleistocene reconstructions (Fig. 5), and the average of  
13 all recent corals is significantly higher than the fossil average value ( $p < 0.05$ ). From these  
14 observations the following three generalizations can be made: (1) the extension rates of the  
15 fossil z-corals are indistinguishable from those of the recent corals, and no distinction exists  
16 between FB and FRT, nearshore and offshore. (2) Bulk density is essentially the same in  
17 recent and fossil Florida z-corals, although some tendency towards higher bulk density as  
18 compared to the fossils may exist. (3) The calcification rates of the recent z-corals are all  
19 higher than those of the fossils (Fig. 5).

20

21 Stable isotope proxy data of the growth environments from the corals used here for  
22 calcification records were described and interpreted in a companion paper (Brachert et al.,  
23 2016) and will not be repeated in detail. For estimates of SSTs, an equation using skeletal  
24  $\delta^{18}\text{O}$  calibrated for *Orbicella* from FRT was applied (Leder et al., 1996) and making the  
25 assumption of a constant value of  $\delta^{18}\text{O}_{\text{water}} = 1.1 \text{ ‰}$  (recent FRT water) for all relevant  
26 interglacials (Brachert et al., 2016). On this basis, we found average annual SSTs between 19



1 and 26 °C which were likely moderated by intermittent upwelling. Reconstructed  
2 temperatures display a negative correlation with annual extension rates ( $p < 0.05$ ) and a  
3 positive relationship with bulk density ( $p < 0.05$ ). In contrast, no clear relation has been found  
4 between SST and calcification rate ( $p > 0.05$ ), although visual inspection suggests an inverse  
5 correlation (Fig. 6). Making other assumptions for  $\delta^{18}\text{O}_{\text{water}}$  (but keeping the value constant  
6 for all specimens) will yield other temperature values, but the range of values between  
7 minima and maxima of average annual temperatures will remain unaffected.

8

### 9 **2.3 Significance of the calcification data**

10 Calcification of z-corals responds to a complex array of environmental factors acting in  
11 concert as to control net calcification (Lough and Cooper, 2011). Next to water temperature,  
12 these factors include water depth, wave exposure, admixtures of “inimical waters” from  
13 carbonate bank interiors, high and low salinity or freshwater discharge, nutrient concentration,  
14 pH and aragonite saturation ( $\Omega_{\text{aragonite}}$ ) (Cohen and Holcomb, 2009; D’Olivio et al., 2014;  
15 Ferrier-Pagès et al., 2000; Ginsburg and Shinn, 1964; Gladfelter et al., 1978; Hofmann et al.,  
16 2011; Johnson and Pérez, 2006; Klein et al., 1993; Lough and Cooper, 2011; Shinn, 1966).  
17 Thus, low calcification rates of the fossil corals can have multiple causes which are eventually  
18 hard to reconstruct. In attempting to sort out small-scale effects along environmental  
19 gradients, patterns related to taxonomy and non-linear calcification responses, we use a big  
20 picture approach beyond environmental gradients and regional acclimatization effects and  
21 compare the reconstructed growth parameters within the frame of measured systems in  
22 southern Florida, the WA and IP (see methods sections for data sources).

23

### 24 **2.4 Environmental effects on calcification in recent and fossil z-corals from** 25 **southern Florida**

1 We use modern analogue data from southern Florida for an evaluation of the calcification  
2 rates documented here for z-corals from Pliocene and Pleistocene units of the Florida  
3 Platform. In southern Florida, environments of z-coral growth range from the salinity stressed  
4 environment of the FB where z-corals only thrive within the most marine parts, to the open  
5 settings of the FRT variably affected by the outflow of “inimical” waters from the interior  
6 bank. Within this region, the highest rates of outflow of bankwater occur in the Middle  
7 Florida Keys where also the lowest calcification rates have been observed (Manzello et al.,  
8 2015a). Negative interference by inimical bank waters with z-coral growth has been  
9 hypothesized, therefore, to be smaller in offshore reefs (>4.5 km from coast) compared to  
10 inshore reefs (<4.5 km from coast). Nonetheless, long-term data averaged from several  
11 *Porites* colonies (Manzello et al., 2015a) do not indicate to a measurable negative spatial  
12 onshore-offshore effect on z-coral calcification. A proximity effect is also not inherent to  
13 the averaged analogue data shown in figure 5: Although low calcification of *Solenastrea* in  
14 FB may be considered compatible with the inimical bank water hypothesis, even lower  
15 calcification rates of *Porites* from an offshore reef is clearly not. Apparently, small-scale  
16 spatial stress effects reported in the literature seem to be averaged out from the big picture.  
17 Because also no difference in calcification responses to environmental effects was found  
18 between *Orbicella cavernosa* and *Porites astreoides* (Manzello et al., 2015a), we consider the  
19 fossil data and recent analog data homogeneous entities not biased by systematic-taxonomical  
20 effects. From this line of reasoning we conclude the low calcification rates of the long-term  
21 fossil record from southern Florida not to reflect a restricted growth environment.

22

## 23 **2.5 Descriptive patterns of calcification in recent and fossil z-corals**

24 The calcification records presented by this study have been classified according to three  
25 descriptive patterns: (1) A negative relationship of extension rate with density being fully  
26 compatible with patterns of recent *Orbicella*. In recent *Porites*, the situation is more complex,

1 because the pattern is documented only in the IP (Lough, 2008), but not in the WA (Elizalde-  
2 Rendon et al., 2010). (2) Extension rate and calcification rate showing a positive relation has  
3 been described also in recent *Porites* from the WA and IP (Elizalde-Rendon et al., 2010;  
4 Lough, 2008), but not in *Orbicella* from the WA which differ by a negative slope (Carricart-  
5 Ganivet, 2004). This is a surprising result, because the skeletal organization of *Solenastrea*  
6 closely resembles that of *Orbicella* and differs significantly from *Porites*, a pattern which was  
7 expected to be reflected in the systematics of calcification. (3) The fossil *Solenastrea* and  
8 recent *Orbicella* and *Porites* display deviating relationships with regard to bulk density and  
9 calcification rates: while the fossil *Solenastrea* shows no relationship, it is positive in  
10 *Orbicella* and WA-*Porites* but negative in IP-*Porites* (Carricart-Ganivet, 2004; Elizalde-  
11 Rendon et al., 2010; Lough, 2008). When plotted against water temperatures, the three  
12 calcification parameters and qualitative trends of the fossils are rather consistent with those of  
13 recent *Orbicella* from the WA (Carricart-Ganivet, 2004), both, in terms of the overall effects  
14 of temperature on extension rate and on bulk density. They differ, however, by the absence of  
15 a temperature control on calcification rates (or the presence of a likely negative slope  
16 according to visual inspection) in the fossils.

17

## 18 **2.6 Comparative analysis of fossil and recent z-coral calcification**

19 Calcification rates recorded by the fossil z-corals are conspicuously low as compared to recent  
20 z-corals from Florida (Fig. 5) which may represent, therefore, possibly no suitable analogue  
21 system. First of all, it should be noted, however, that the calcification data from the fossil  
22 *Solenastrea* (plus *Orbicella* and *Porites*) appear to be from a larger window of average annual  
23 temperatures ( $\sim 7^\circ\text{C}$ ) than covered by field studies on recent z-coral growth. Temperature  
24 differences behind growth data from southern Florida are rather small, and even growth data  
25 collected in the Gulf of Mexico and the Caribbean Sea both cover small gradients of average  
26 annual SSTs ( $\sim 1^\circ\text{C}$ ) where *Orbicella* (*Orbicella annularis*) display positive calcification

1 responses with increasing SST (Carricart-Ganivet, 2004). Although calcification rates are the  
2 same in both regions, average annual SSTs differ by  $\sim 2$  °C and likely reflect the  
3 acclimatization of the same morphological taxon to regionally different SST regimes. Thus,  
4 acclimatization effects on calcification seem to play a role within rather small observational  
5 scales. Within the same region, another species of the same genus (*Orbicella falveolata*),  
6 however, responds with declining calcification to this subtle gradient of  $\sim 1$ °C of average  
7 annual SST change (Carricart-Ganivet et al., 2012), either because acclimatization is not yet  
8 fully accomplished, or because the SST regime is near the upper threshold of ecological  
9 tolerance of *O. falveolata* allowing no further positive acclimatization. We assume, the latter  
10 is more likely and, therefore, calcification responses to SST seem to be non-linear over the  
11 full range of ecological tolerance of this and other taxa. This sort of non-linear responses of  
12 calcification has been predicted by a modeling study on the ecological tolerance of *Orbicella*  
13 over a temperature window of 3 – 4 °C (Worum et al., 2007) and is also well documented by  
14 comprehensive field studies on *Porites* from the Great Barrier Reef system (IP) (Cooper et al.,  
15 2008; De'ath et al., 2013; De'ath et al., 2009). The tipping point between increases and  
16 decreases of calcification rates was found to be between 26 °C and 27 °C for *Porites* and  
17 *Orbicella* (Carricart-Ganivet et al., 2012; Cooper et al., 2008), or 28 – 29 °C according to  
18 modeling (Worum et al., 2007). This kind of large-scale observational data seems essential for  
19 interpreting fossil calcification data and, therefore, we discuss the calcification data in the  
20 context of the entire WA and IP.

21

### 22 2.6.1 Florida and Western Atlantic

23 Within the larger context of the WA, all parameters of calcification are higher in the recent z-  
24 corals than in the fossil z-corals. The extension rates of the fossils with a mean of  $0.44 \pm 0.19$   
25  $\text{cm yr}^{-1}$  and ranging from 0.16 to 0.86  $\text{cm yr}^{-1}$  contrast with substantially higher mean values  
26 of  $0.79 \pm 0.31$   $\text{cm yr}^{-1}$  and ranges between 0.28  $\text{cm yr}^{-1}$  and 1.44  $\text{cm yr}^{-1}$  in the recent WA

1 (Fig. 7; Tab. 3). Bulk density of the fossil z-corals displays a variability comparable to that of  
2 recent z-corals but the average from all fossil specimens ( $0.86 \pm 0.22 \text{ g cm}^{-3}$ ) is substantially  
3 lower than in the recent z-corals ( $1.37 \pm 0.24 \text{ g cm}^{-3}$ ) from the WA in our database (Fig. 7,  
4 Tab. 3). Maximum values ( $1.22 \text{ g cm}^{-3}$ ) are lower than in the modern ( $1.94 \text{ g cm}^{-3}$ ) and  
5 minimum values of  $0.55 \text{ g cm}^{-3}$  are also below minimum values of recent WA z-corals ( $0.78 \text{ g}$   
6  $\text{cm}^{-3}$ ; Tab. 3). Calcification rates inferred from this set of inputs for any give extension rate  
7 are ~50 % lower than those from modern z-corals.

8  
9 The recent data from the WA are from the four genera (listed according to the number of data  
10 available) *Orbicella*, *Porites*, *Diploria/Pseudodiploria* and *Solenastrea*, however, and some of  
11 the discrepancy between fossils and recent z-corals, may therefore be an artifact of the  
12 database. When compared on the taxonomical genus level, extension rates of *Porites* (range =  
13 0.28 to 0.48, mean =  $0.37 + 0.07 \text{ cm yr}^{-1}$ ) and *Diploria/Pseudodiploria* (range = 0.30 to 0.40,  
14 mean =  $0.35 + 0.04 \text{ cm yr}^{-1}$ ) are significantly lower than those of *Orbicella* (range = 0.38 to  
15 1.44, mean =  $0.91 \pm 0.23 \text{ cm yr}^{-1}$ ,  $p < 0.05$ ) but are identical with regard to density (*Porites*:  
16 range = 1.10 to 1.72, mean =  $1.44 \pm 0.20 \text{ g cm}^{-3}$ ; *Diploria*: range = 0.97 to 1.70; mean =  $1.27 \pm$   
17  $0.31 \text{ g cm}^{-3}$ ; *Orbicella*: range = 0.78 to 1.94, mean =  $1.37 \pm 0.24 \text{ g cm}^{-3}$ ;  $p > 0.05$ ). *Orbicella*  
18 display a negative relationship between extension rate and bulk density ( $R^2 = 0.27$ ,  $p < 0.05$ ),  
19 whereas no such relationship has been documented for *Porites* ( $R^2 = 0.30$ ,  $p > 0.05$ ) and  
20 *Diploria/Pseudodiploria* ( $R^2 = 0.11$ ,  $p > 0.05$ ) which are indistinguishable in their calcification  
21 data (Fig. 7). Remarkably, *Porites* and *Diploria/Pseudodiploria* are indistinguishable not only  
22 with regard to their general calcification relationship but also quantitatively in terms of  
23 absolute values and clearly differ from those of *Orbicella*, whose calcification rates are  
24 significantly higher at almost any given density (Fig. 7). *Solenastrea* is unusual due to its low  
25 extension rates (range = 0.22 to 0.58, mean =  $0.43 \pm 0.19 \text{ cm yr}^{-1}$ ) and low bulk density (range  
26 = 0.55 to 1.22, mean =  $0.88 \pm 0.22 \text{ g cm}^{-3}$ ). Like *Orbicella*, extension rate and bulk density

1 display a significant negative relationship ( $R^2 = 0.23$ ,  $p < 0.05$ ), whereas extension rate is  
2 positively correlated with calcification rate ( $R^2 = 0.47$ ,  $p < 0.05$ ). Bulk density, on the other  
3 hand, displays no correlation with calcification rate ( $R^2 = 0.06$ ,  $p > 0.05$ ).

4  
5 For the relationships described above, we find no consistent patterns of the parameters of  
6 calcification between recent and fossil specimens and between taxa. While the data from the  
7 recent *Solenastrea* specimen is similar to the data from fossil *Solenastrea* (Fig. 7), the single  
8 fossil *Porites* available is incompatible with recent *Porites* from the WA, both in terms of  
9 extension rate and bulk density, but plots together with fossil *Solenastrea* (Fig. 7). Also, the  
10 Pliocene *Diploria/Pseudodiploria* (only extension rates available from literature data) clearly  
11 differ from their recent counterparts with significantly higher extension rates (Fig. 7). With  
12 regard to *Orbicella*, bulk density of the two fossil specimens available is lower at any given  
13 extension rate than in the recent *Orbicella*, but consistent with fossil *Solenastrea* (Fig. 7). In  
14 extension rate vs. bulk density space, we observe a duality between recent and fossil z-corals,  
15 rather than any taxonomical distinction. With regard to calcification rates, fossils also have  
16 lower values at any given extension rate than recent z-corals (Fig. 7). On the other hand, no  
17 clear separation exists between fossils and recent z-corals with regard to bulk density vs.  
18 calcification rate because of very high extension rates of *Orbicella* compared to the other taxa  
19 (Fig. 7). In contrast to field studies having demonstrated calcification systematics of reef  
20 corals to differ between the genera *Orbicella* of the WA and *Porites* of the IP (Carricart-  
21 Ganivet, 2004; Lough, 2008), systematics of calcification of z-corals seem, therefore, to  
22 depend also on ocean regions or coral provinces.

23

#### 24 2.6.2 Indo-Pacific

25 Extension rates of recent z-corals documented by our literature review for the WA (various  
26 taxa) and IP (*Porites* only) have a broad range of values from 0.28 to 2.38  $\text{cm yr}^{-1}$ , however,

1 z-corals of the WA have significantly lower mean extension rates ( $0.28 - 1.44$ , mean:  $0.79 \pm$   
2  $0.31 \text{ cm yr}^{-1}$ ) than those of the IP ( $0.30 - 2.38$ , mean:  $1.28 \pm 0.50 \text{ cm yr}^{-1}$ ,  $p < 0.05$ ; Tab. 3).  
3 Fossil corals have lower values than the recent corals ( $0.16 - 0.89$ , mean:  $0.45 \pm 0.20 \text{ cm yr}^{-1}$ ,  
4  $p < 0.05$ ), including those from the WA, and some of the fossils have the smallest values  
5 recorded (Fig. 8A). With regard to density, there is a broad range of values; however, no  
6 significant difference exists among the WA ( $0.78 - 1.94$ , mean:  $1.37 \pm 0.24 \text{ g cm}^{-3}$ ) and IP z-  
7 corals ( $1.01 - 1.90$ , mean:  $1.30 \pm 0.16 \text{ g cm}^{-3}$ ,  $p > 0.05$ ), although the range of values is larger  
8 in the WA. Fossil corals have a similar range but clearly have significantly lower bulk density  
9 than the recent corals ( $p < 0.05$ ) and also have the lowest minimum values of bulk density  
10 recorded ( $0.55 - 1.22$ , mean:  $0.86 \pm 0.22 \text{ g cm}^{-3}$ ; Tab. 2). The recent z-corals of the WA and  
11 IP show significant negative correlations between extension rate and density with an identical  
12 slope (F-test;  $p < 0.05$ ) and intercept. While the correlation in the IP z-coral data is highly  
13 significant ( $R^2 = 0.52$ ,  $p < 0.05$ ) it is weaker but still significant in the WA data ( $R^2 = 0.14$ ,  $p <$   
14  $0.05$ ; Fig. 8A). The fossil reef corals show a significant negative relationship between  
15 extension rate and bulk density defined by linear regression as well, but the slope is steeper  
16 (F-test;  $p > 0.05$ ) than in the recent corals ( $R^2 = 0.43$ ,  $p < 0.05$ ) (Fig. 8A).  
17  
18 Calcification rates of z-corals have a large range of values from  $0.18$  to  $2.82 \text{ g cm}^{-2} \text{ yr}^{-1}$  (Tab.  
19 2). In recent and fossil z-corals, there is a significant positive correlation between extension  
20 and calcification rate ( $p < 0.05$ ). In recent WA-corals, calcification rates ( $0.31 - 1.78$ , mean:  
21  $1.06 \pm 0.38 \text{ g cm}^{-2} \text{ yr}^{-1}$ ) remain clearly below those of the IP ( $0.56 - 2.82$ , mean:  $1.67 \pm 0.49$   
22  $\text{cm}^{-2} \text{ yr}^{-1}$ ) because of higher extension rates. Importantly, the slope of the relationship is  
23 identical (F-test;  $p < 0.05$ ) in the WA and IP and the relationships are highly significant ( $R^2 =$   
24  $0.93$  and  $0.70$ ,  $p < 0.05$ , respectively), whereas the slope of the relationship is smaller by  $\sim 50$   
25 % (F-test;  $p > 0.05$ ) in the fossil corals (Fig. 8B). No such simple relationships exist between  
26 density and calcification rate. In the IP, there is a significant negative relation between density

1 and calcification ( $R^2= 0.32$ ,  $p < 0.05$ ), whereas in the WA, there is no relationship ( $R^2= 0.00$ ,  
2  $p > 0.05$ ; Fig. 8C). Therefore, variations in calcification rates in the latter region are entirely  
3 driven by changes in extension rates, whereas in the IP, it is driven by both extension rates  
4 and bulk density, and decreasing density weakens the effect of increased extension on  
5 calcification. In the data from the Florida fossils no relationship of density was found with  
6 calcification rate ( $R^2 = 0.02$ ,  $p > 0.05$ ) which means that changes of calcification rate fully  
7 depend on variable extension and the pattern in essence resembles that of the WA (Fig. 8B,  
8 C).

9  
10 Importantly, the recent z-corals from the WA display significantly lower values and a smaller  
11 range of values of all three calcification parameters (extension rate, bulk density, calcification  
12 rate) compared to the z-corals from the IP (Fig. 8D-F, Tab. 2). This corresponds with different  
13 temperature windows of z-coral distribution in the database. The WA corals in the database  
14 cover a rather small range of average annual temperature between 26.4 and 28.6 °C, whereas  
15 the IP z-corals represent the spectrum of average annual water temperature between 23.0 and  
16 29.6 °C. Within these two temperature windows, differences between the WA and IP corals  
17 also pertain to patterns: In the IP, extension rates show a marked increase but bulk density  
18 decreases which combines to present a positive relationship of calcification rate with  
19 temperature. No such relationship exists in the WA corals (Fig. 8). Because of the established  
20 non-linearity of life processes in poikilothermic biota alike the reef corals (Goreau and  
21 Macfarlane, 1990; Grizzle et al., 2001; Townsend et al., 2008) linear regression is likely  
22 inappropriate for describing the statistics of calcification within the temperature windows  
23 documented by the data and beyond (Fig. 8D-F) and we have alternatively applied a quadratic  
24 polynomial to the data. With respect to the WA data, this procedure results in an inverted  
25 parabolic relationship of extension rate with temperature ( $p < 0.05$ ). Corresponding parabolic  
26 regressions for density and calcification rate are not significant ( $p > 0.05$ ), however, and may



1 be an effect of rather poor resolution of the temperature data in the database. The relationship  
2 is consistent with calcification data from regional studies (Carricart-Ganivet, 2004; Carricart-  
3 Ganivet et al., 2012), but on a large scale.

4

### 5 **3 Lessons from the recent analogue**

6 Although maximum extension rates in the IP are higher than those recorded in the WA, the  
7 overall relationship with density (slope and intercept of the regression) can be regarded as  
8 identical (Fig. 8). Recent z-corals from the WA display enhanced variability of bulk density  
9 associated with low extension rates, which results from the noisy inputs of  
10 *Diploria/Pseudodiploria* and *Porites*, whereas *Orbicella* forms a consistent population like  
11 *Porites* in the IP (Fig. 7, 8). It should be noted, that the slope of linear regression is steeper in  
12 WA-*Orbicella* than IP-*Porites* according to an F-test ( $p < 0.05$ ) (Fig. 5, 7A). In contrast, the  
13 Florida fossil z-corals have significantly lower extension rates and mean bulk densities than  
14 all of their recent counterparts, and also have an extension rate / density relationship which  
15 differs from that of all recent z-corals in the database ( $p < 0.05$ ) (Fig. 6).

16

17 With regard to calcification rates, all recent corals display an identical relationship between  
18 extension rate and calcification, irrespective of taxon or provenance, and this relationship is  
19 significantly different from that of the fossils (F-test  $p < 0.05$ ) (Fig. 8B). The relationships of  
20 bulk density with calcification rate, however, significantly differ in the populations from the  
21 recent WA, the IP, and the Plio-Pleistocene of Florida, respectively (Fig. 8C).

22

23 From this discussion we conclude that recent and fossil z-corals clearly differ with regard to  
24 their relationships of extension rate with bulk density and that taxonomical peculiarities seem  
25 not to play a significant role for the big picture (Fig. 7, 8A). We further conclude, that the  
26 relationship of extension rate with calcification rate is identical in recent z-corals from all

1 ocean regions, but is significantly different between recent and fossil z-corals (Fig. 7B). Bulk  
2 density and calcification rate, on the other hand, display individual traits among the recent z-  
3 corals from the WA, the IP and the Plio-Pleistocene of Florida (Fig. 8C).

4  
5

### 6 **3.1 Low calcification rates due to high nutrients or low $\Omega_{\text{aragonite}}$ ?**

7 Field studies on z-coral skeletal accretion found calcification rates to be closely coupled with  
8 the saturation state of seawater with respect to aragonite ( $\Omega_{\text{aragonite}}$ ). These laboratory studies  
9 found z-corals not to acclimatize to short-term changes in  $\Omega_{\text{aragonite}}$  and calcification rates to  
10 decline with decreasing  $\Omega_{\text{aragonite}}$  (Cohen and Holcomb, 2009; Gattuso et al., 1998; Langdon et  
11 al., 2000). Cool upwelling waters have a number of adverse effects on z-coral growth, namely  
12 low pH/low  $\Omega_{\text{aragonite}}$  of ambient water (Furnas, 2011). In our fossil materials, z-coral  
13 skeletons recording maximum upwelling according to their stable isotope composition, have  
14 the smallest density values but largest values of extension rate (Brachert et al., 2016). This  
15 conforms with findings from the Galapagos upwelling system, where z-coral skeletal density is  
16 reduced under maximum upwelling stresses, but extension rate is higher than predicted from  
17 the ambient SST (Manzello et al., 2014). In an upwelling regime, the low volumes of cements  
18 in intra-skeletal porosity of the corals and the low degree of cementation of the shallow-  
19 marine carbonates may reflect the effects of phosphate poisoning (Hallock and Schlager,  
20 1986; Manzello et al., 2014), but the benthic assemblages and low amounts of bioerosion do  
21 not provide compelling evidence for high eutrophy. If any, these findings support intermittent  
22 upwelling which has positively interfered with z-coral calcification on the Florida platform  
23 during the Plio-Pleistocene, but clearly documents minimal calcification rates to have  
24 coincided with episodes with minimum upwelling (Brachert et al., 2016). Thus, the latter  
25 cannot be the prime reason for the observed low calcification rates.

1  
2 Furthermore, the low extension rates of the Plio-Pleistocene z-corals from Florida are fully  
3 compatible with those published from fossil z-corals at various locations in the tropical WA  
4 (various taxa) which also range between 0.3 and 0.8 cm yr<sup>-1</sup> during the Pliocene (Johnson and  
5 Pérez, 2006), ~0.3 cm yr<sup>-1</sup> in the late Miocene (Denniston et al., 2008b) and 0.2 and 1.0 cm yr<sup>-1</sup>  
6 in the FRT during the late Pleistocene (0.13 Ma) (Gischler et al., 2009) (Fig. 7G). For this  
7 reason, low extension rates recorded by the Florida fossils are representative of the entire  
8 tropical WA at that time and were as such a large-scale regional or global phenomenon. The  
9 saturation of the sea water with CaCO<sub>3</sub> has been shown to be an environmental factor  
10 controlling calcification rates in z-corals (Langdon et al., 2000), and causes for globally low  
11 pH/low  $\Omega_{\text{aragonite}}$  in ambient water may be sought in high atmospheric  $p\text{CO}_2$  levels. Low  
12 calcification rates of the Florida corals may, therefore, be an effect of high  $p\text{CO}_2$  during the  
13 Plio-Pleistocene interglacials. However, for the last 3 Ma after the mid Pliocene climatic  
14 optimum (~3 Ma), reconstructed  $p\text{CO}_2$  was near pre-industrial levels and only during and  
15 before the climatic optimum was at the levels predicted to exist by the end of this century  
16 (IPCC, 2013; Seki et al., 2010). For the long-term buffering effect of the ocean,  $\Omega_{\text{aragonite}}$  has  
17 been suggested to have been not significantly different from the present day, however  
18 (Hönisch et al., 2012). Substantial  $p\text{CO}_2$  changes have been documented over the glacial /  
19 interglacial cycles of the Quaternary (Petit et al., 1999), concomitant with changes in  
20 calcification of calcareous plankton (Barker and Elderfield, 2002; Beaufort et al., 2011), and  
21 may be, for these reasons, a potential driver of the observed low calcification rates.

22

### 23 **3.3 Low calcification rates due to heat stress?**

24 Next to  $\Omega_{\text{aragonite}}$ , temperature is an important control of z-coral calcification in the world  
25 oceans. Given the simplification in our reconstruction of SSTs discussed above, the extension  
26 rates still display a negative correlation with the average annual SST ( $p < 0.05$ ) and bulk

1 density a positive relationship with SST ( $p < 0.05$ ). In contrast, no clear relation has been  
2 found between SST and calcification rate ( $p > 0.05$ ), although visual inspection suggests an  
3 inverse correlation (Fig. 8). This pattern is qualitatively rather consistent with recent  
4 *Orbicella* (Carricart-Ganivet, 2004), however, at a substantially larger temperature window in  
5 the fossil material and an absent relationship or likely negative correlation of calcification rate  
6 with temperature (Fig. 6).

7  
8 Over the large temperature window of 6.9 °C covered by the modern IP data, a pattern of  
9 changes driven by temperature has been documented using linear regression (Fig. 8D-F). In  
10 contrast, the temperature range documented by z-corals from the WA database covers only  
11 2.2 °C (Fig. 8D-F) and calcification data do not display any linear relationship. Instead of a  
12 linear fit, they can be approximated using a quadratic polynomial which should suggest the  
13 present temperature window realized by recent z-corals of the WA to cover more or less the  
14 ecological spectrum of this coral province. Low extension rates documented by fossil z-corals  
15 from Florida and many other locations of the Caribbean, therefore, potentially document  
16 temperatures either near their lower or upper levels of ecological tolerance. In our temperature  
17 reconstruction using skeletal  $\delta^{18}\text{O}$  values, we apply a value of  $\delta^{18}\text{O}_{\text{water}}$  which likely  
18 underestimates the actual SST because other methods consistently found SSTs of the WA  
19 warm pool  $\sim 2$  °C above present values during the last 5 Ma (Fedorov et al., 2013; O'Brien et  
20 al., 2014). Low calcification rates in z-corals may, therefore, reflect warmer-than-present  
21 SSTs during the Plio-Pleistocene interglacials. Such an interpretation is consistent with  
22 concepts of nonlinear calcification responses to temperature in z-corals (Brachert et al., 2013;  
23 Gischler et al., 2009; Worum et al., 2007). Correspondingly, approaches describing coral  
24 calcification within temperature windows of  $\leq 1$  °C of annual temperature would not describe  
25 z-coral calcification over the full spectrum of ecological tolerance of a given species and may  
26 describe calcification near the optimum or lower / upper threshold of calcification only. In

1 application of this concept, z-coral growth in the WA was likely under significant heat stress,  
2 and annual water temperatures 2 °C higher than at present were causing calcification rates 50  
3 % lower than present day. It should be noted also, that upwelling has been ascribed a  
4 mitigating effect on SST stresses depending on the depth of upwelling or the timing during  
5 the year (Chollett et al., 2010; Riegl and Piller, 2003) and maximum extension rates /  
6 minimum density of the Florida z-corals coincided with a maximum of upwelling.  
7 Intermittent upwellings during the Plio-Pleistocene, therefore, seem to have created temporary  
8 refuges for z-corals by episodically mitigating heat stresses (Brachert et al., 2016). This  
9 finding supports notions of hot SSTs during the Eemian interglacial to have resulted in reef  
10 kills at equatorial latitudes and poleward migrations of many z-coral taxa (Kiessling et al.,  
11 2012). Our data also suggest recent coral reefs at equatorial latitudes to be potentially  
12 endangered from rising SSTs with ongoing climate change and ocean acidification (IPCC,  
13 2013).

14

#### 15 **4 Conclusions**

- 16 • This study presents the first quantitative record of calcification rates from fossil reef  
17 corals (z-corals).
- 18 • Z-coral skeletons from Pliocene and Pleistocene precursors of the modern Florida  
19 carbonate platform display pristine preservation of stable isotope signatures and  
20 calcification data.
- 21 • Extension rates of Plio-Pleistocene specimens from Florida (various taxa) are  
22 remarkably low, but compatible with those of other tropical Caribbean settings at that  
23 time.
- 24 • Calcification data are undistinguishable among geological time-slices (interglacials),  
25 but bulk density and calcification rate of recent z-corals from Florida are remarkably  
26 high compared to the fossils.

- 1       • Average calcification rates of Pliocene and Pleistocene specimens, irrespective of z-  
2 coral taxon, were only 50% of the recent values in the WA.
- 3       • The reasons behind low calcification rates during the Plio-Pleistocene interglacials are  
4 not clear but a lower-than-recent saturation of seawater with aragonite or high water  
5 temperatures near the limits of ecological tolerance are likely candidates.

6  
7

### 8   **Acknowledgements**

9   Eduard Petuch (Florida Atlantic University, USA) provided some of the samples needed for  
10 this study. Kurt Schubert carefully prepared the coral slices and Jörg Lenzner made the SEM  
11 micrographs (both University of Leipzig, Germany). Adrian Immenhauser (University of  
12 Bochum, Germany) made valuable comments to an earlier manuscript. Funding by the  
13 Deutsche Forschungsgemeinschaft is gratefully acknowledged (BR 1153/13-1).

14

### 15   **Author contribution**

16   TCB designed this research; field work was carried out by TCB, MR and JSK. Laboratory analyses  
17 were performed by TCB, SK and MR. KH provided calcification records from a recent *Solenastrea*  
18 from Florida Bay. TCB, MR and JML wrote the paper.

## 1 References

- 2 Allison, N., Finch, A. A., and EIMF:  $\delta^{11}\text{B}$ , Sr, Mg and B in a modern *Porites* coral: the relationship  
3 between calcification site pH and skeletal chemistry, *Geochimica Cosmochimica Acta*, 79, 1970-1800,  
4 2010.
- 5 Allison, N., Finch, A. A., Webster, J. M., and Clague, D. A.: Palaeoenvironmental records from fossil  
6 corals: The effects of submarine diagenesis on temperature and climate estimates, *Geochimica et*  
7 *Cosmochimica Acta*, 71, 4693-4703, 2007.
- 8 Allmon, W. D.: Nutrients, temperature, disturbance, and evolution: a model for the late Cenozoic  
9 marine record of the western Atlantic, *Palaeogeography, Palaeoclimatology, Palaeoecology*, 166, 9-26,  
10 2001.
- 11 Allmon, W. D., Spizuco, M. P., and Jones, D. S.: Taphonomy and paleoenvironment of two turritellid-  
12 gastropod-rich beds, Pliocene of Florida, *Lethaia*, 28, 75-83, 1995.
- 13 Anagnostou, E., Sherrell, R. M., Gagnon, A., LaVigne, M., Field, M. P., and McDonough, W. F.:  
14 Seawater nutrient and carbonate ion concentrations recorded as P/Ca, Ba/Ca, and U/Ca in the deep-sea  
15 coral *Desmophyllum dianthus*, *Geochimica et Cosmochimica Acta*, 75, 2529-2543, 2011.
- 16 Baker, P. A. and Weber, J. N.: Coral growth rate: Variation with depth, *Earth and Planetary Science*  
17 *Letters*, 27, 57-61, 1975.
- 18 Barker, C. E.: Fluid inclusions in the Pleistocene Miami Limestone, southeastern Florida: potentially  
19 misleading evidence of vadose diagenesis [abs.], *Geological Society of America, Abstracts with*  
20 *Programs*, 20, A119, 1986.
- 21 Barker, S. and Elderfield, H.: Foraminiferal Calcification Response to Glacial-Interglacial Changes in  
22 Atmospheric CO<sub>2</sub>, *Science*, 297, 833-836, 2002.
- 23 Bathurst, R. G. C.: *Carbonate Sediments and their Diagenesis*, Elsevier Science Publ. Co., New York,  
24 1975.
- 25 Beaufort, L., Probert, I., de Garidel-Thoron, T., Bendif, E. M., Ruiz-Pino, D., Metzl, N., Goyet, C.,  
26 Buchet, N., Coupel, P., Grelaud, M., Rost, B., Rickaby, R. E. M., and de Vargas, C.: Sensitivity of  
27 coccolithophores to carbonate chemistry and ocean acidification, *Nature*, 476, 80-83, 2011.
- 28 Bessat, F. and Buigues, D.: Two centuries of variation in coral growth in a massive *Porites* colony  
29 from Moorea (French Polynesia): a response of ocean-atmosphere variability from south central Pacific,  
30 *Palaeogeography, Palaeoclimatology, Palaeoecology*, 175, 381-392, 2001.
- 31 Böcker, A.: Interannual and seasonal climate variability recorded by reef corals, Plio/Pleistocene  
32 (Florida) and Mio/Pliocene (Dominican Republic), Dissertation, Fakultät für Physik und  
33 Geowissenschaften, Universität Leipzig, Leipzig, 2014.
- 34 Brachert, T. C., Reuter, M., Felis, T., Kroeger, K. F., Lohmann, G., Micheels, A., and Fassoulas, C.:  
35 *Porites* corals from Crete (Greece) open a window into Late Miocene (10 Ma) seasonal and  
36 interannual climate variability, *Earth and Planetary Science Letters*, 245, 81-94, 2006a.
- 37 Brachert, T. C., Reuter, M., Kroeger, K. F., and Lough, J.: Coral growth bands: A new and easy to use  
38 paleothermometer in paleoenvironment analysis and paleoceanography (late Miocene, Greece),  
39 *Paleoceanography* 21, PA4217, 2006b. 2006b.
- 40 Brachert, T. C., Reuter, M., Krüger, S., Böcker, A., Lohmann, H., Mertz-Kraus, R., and Fassoulas, C.:  
41 Density banding in corals: barcodes of past and current climate change, *Coral Reefs*, 32, 1013-1023,  
42 2013.
- 43 Brachert, T. C., Reuter, M., Krüger, S., Kirkerowicz, J., and Klaus, J. S.: Plio-/Pleistocene upwellings  
44 mitigated heat stress for reef corals on the Florida platform (USA), *Biogeosciences*, 12, 16553-16602,  
45 2016.
- 46 Brachert, T. C., Reuter, M., Krüger, S., Lohmann, H., Petuch, E. J., and Klaus, J. S.: A 4.2 Million  
47 years record of interglacial paleoclimate from sclerochronological data of Florida carbonate platform  
48 (Early Pliocene to recent), *Global and Planetary Change*, 120, 54-64, 2014.
- 49 Budd, A. F., Fukami, H., Smith, N. D., and Knowlton, N.: Taxonomic classification of the reef coral  
50 family *Mussidae* (Cnidaria: Anthozoa: Scleractinia), *Zoological Journal of the Linnean Society*, 166,  
51 465-529, 2012.
- 52 Cantin, N. E., Cohen, A. L., Karnauskas, K. B., Tarrant, A. M., and McCorkle, D. C.: Ocean warming  
53 slows coral growth in the central Red Sea, *Science*, 329, 322-325, 2010.

1 Carricart-Ganivet, J. P.: Sea surface temperature and the growth of the West Atlantic reef-building  
2 coral *Montastraea annularis*, *Journal of Experimental Marine Biology and Ecology*, 302, 249-260,  
3 2004.

4 Carricart-Ganivet, J. P., Beltrán-Torres, A. U., Merino, M., and Ruiz-Zárate, M. A.: Skeletal  
5 extension, density and calcification rate of the reef building coral *Montastraea annularis* (Ellis and  
6 Solander) in the Mexican Caribbean, *Bulletin of Marine Science*, 66, 215-224, 2000.

7 Carricart-Ganivet, J. P., Cabanillas-Terán, N., Cruz-Ortega, I., and Blanchon, P.: Sensitivity of  
8 calcification to thermal stress varies among genera of massive reef-building corals, *PLoS ONE*, 7, 1-8,  
9 2012.

10 Carricart-Ganivet, J. P. and Merino, M.: Growth responses of the reef-building coral *Montastraea*  
11 *annularis* along a gradient of continental influence in the southern Gulf of Mexico, *Bulletin of Marine*  
12 *Science*, 68, 133-146, 2001.

13 Chollett, I., Mumby, P. J., and Cortes, J.: Upwelling areas do not guarantee refuge for coral reefs in a  
14 warming world, *Marine Ecology Progress Series*, 416, 47-56, 2010.

15 Cohen, A. L. and Holcomb, M.: Why corals care about ocean acidification. Uncovering the  
16 mechanism, *Oceanography*, 22, 118-127, 2009.

17 Constantz, B. R.: The primary surface area of corals and variations in their susceptibility to diagenesis.  
18 In: *Reef Diagenesis*, Schroeder, J. H. and Purser, B. H. (Eds.), Springer-Verlag, New York, 1986.

19 Cooper, T. F., De'Ath, G., Fabricius, K. E., and Lough, J. M.: Declining coral calcification in massive  
20 *Porites* in two nearshore regions of the northern Great Barrier Reef, *Global Change Biology*, 14, 529-  
21 538, 2008.

22 D'Olivio, J. P., McCulloch, M. T., Eggins, S. M., and Trotter, J.: Coral records of reef-water pH  
23 across the central Great Barrier Reef, Australia: assessing the influence of river runoff on inshore  
24 reefs, *Biogeosciences Discussions*, 11, 11443-11479, 2014.

25 De'ath, G., Fabricius, K., and Lough, J.: Yes — Coral calcification rates have decreased in the last  
26 twenty-five years!, *Marine Geology*, 346, 400-402, 2013.

27 De'ath, G., Lough, J. M., and Fabricius, K. E.: Declining Coral Calcification on the Great Barrier Reef,  
28 *Science*, 323, 116-119, 2009.

29 Denniston, R. F., Asmeron, Y., Polyak, V. Y., McNeill, D., Klaus, J. S., Cole, P., and Budd, A. F.:  
30 Caribbean chronostratigraphy constrained with U-Pb and <sup>87</sup>Sr/<sup>86</sup>Sr analysis of a Miocene coral,  
31 *Geology*, 36, 151-153, 2008a.

32 Denniston, R. F., Penn, S. C., and Budd, A. F.: Constraints on Late Miocene shallow marine  
33 seasonality for the Central Caribbean using oxygen isotopes and Sr/Ca ratios in a fossil coral. In:  
34 *Evolutionary stasis and change in the Dominican Republic Neogene*, Nehm, R. H. and Budd, A. F.  
35 (Eds.), *Topics in Geobiology*, 30, Springer Science and business Media B.V., Heidelberg, 2008b.

36 Dodge, R. E. and Brass, G. W.: Skeleton extension, density and calcification of the reef coral  
37 *Montastrea annularis*: St. Croix, U.S. Virgin Islands, *Bulletin of Marine Science*, 34, 288-307, 1984.

38 Dowsett, H. J. and Cronin, T. M.: High eustatic sea level during the middle Pliocene: Evidence from  
39 the southeastern U.S. Atlantic Coastal Plain, *Geology*, 18, 435-438, 1990.

40 Dullo, W.-C.: Progressive diagenetic sequence of aragonite structures: Pleistocene coral reefs and their  
41 modern counterparts on the eastern Red Sea coast, Saudi Arabia, *Palaeontographica Americana*, 54,  
42 254-160, 1984.

43 Dustan, P.: Growth and form in the reef-building coral *Montastrea annularis*, *Marine Biology*  
44 (Berlin), 33, 101-107, 1975.

45 Elizalde-Rendon, E. M., Horta-Puga, G., Gonzalez-Diaz, P., and Carricart-Ganivet, J. P.: Growth  
46 characteristics of the reef-building coral *Porites astreoides* under different environmental conditions in  
47 the Western Atlantic, *Coral Reefs*, 29, 607-614, 2010.

48 Emslie, S. D. and Morgan, G. S.: A Catastrophic Death Assemblage and Paleoclimatic Implications of  
49 Pliocene Seabirds of Florida, *Science*, 264, 684-685, 1994.

50 Fabricius, K. E., Langdon, C., Uthicke, S., Humphrey, C., Noonan, S., De'ath, G., Okazaki, R.,  
51 Muehllehner, N., Glas, M. S., and Lough, J. M.: Losers and winners in coral reefs acclimatized to  
52 elevated carbon dioxide concentrations, *Nature Clim. Change*, 1, 165-169, 2011.

53 Fedorov, A. V., Brierley, C. M., Lawrence, K. T., Liu, Z., Dekens, P. S., and Ravelo, A. C.: Patterns  
54 and mechanisms of early Pliocene warmth, *Nature*, 496, 43-49, 2013.



1 Felis, T., Lohmann, G., Kuhnert, H., Lorenz, S. J., Scholz, D., Pätzold, J., Al-Rousan, S. A., and Al-  
2 Moghrabi, S. M.: Increased seasonality in Middle East temperatures during the last interglacial period,  
3 Nature, 429, 164-168, 2004.

4 Felis, T. and Pätzold, J.: Climate reconstructions from annually banded corals. In: Global  
5 environmental change in the ocean and on land, Shiyomi, M., Kawahata, H., Koizumi, H., Tsuda, A.,  
6 and Awaya, Y. (Eds.), Terrapub, Tokyo, 2004.

7 Ferrier-Pagès, C., Gattuso, J.-P., Dallot, S., and Jaubert, J.: Effect of nutrient enrichment on growth  
8 and photosynthesis of the zooxanthellate coral *Stylophora pistillata*, Coral Reefs, 19, 103-113, 2000.

9 Flügel, E.: Microfacies analysis of carbonate rocks. Analysis, interpretation and application., Springer  
10 Verlag, Heidelberg, 2004.

11 Furnas, J.: Upwelling and coral reefs. In: Encyclopedia of modern coral reefs - structure, form and  
12 process, Hopley, D. (Ed.), Encyclopedia of earth sciences series, Springer, Dordrecht, 2011.

13 Gattuso, J.-P., Frankignoulle, M., Bourge, I., Romaine, S., and Buddemeier, R. W.: Effect of calcium  
14 carbonate saturation of seawater on coral calcification, Global and Planetary Change, 18, 37-46, 1998.

15 Ginsburg, R. N. and Shinn, E. A.: Distribution of the reef-building community in Florida and the  
16 Bahamas [abs.], American Association of Petroleum Geologists Bulletin, 48, 527, 1964.

17 Gischler, E., Hudson, J., and Storz, D.: Growth of Pleistocene massive corals in south Florida: low  
18 skeletal extension-rates and possible ENSO, decadal, and multi-decadal cyclicities, Coral Reefs, 28,  
19 823-830, 2009.

20 Gladfelter, E. H., Monahan, R. K., and Gladfelter, W. B.: Growth rates of five reef-building corals in  
21 the northeastern Caribbean, Bulletin of Marine Science, 28, 728-734, 1978.

22 Goodkin, N. F., Switzer, A. D., McCorry, D., DeVantier, L., D. True, J. D., Hughen, K. A., Angeline,  
23 N., and Yang, T. T.: Coral communities of Hong Kong: long-lived corals in a marginal reef  
24 environment, Marine Ecology Progress Series, 426, 185-196, 2011.

25 Goreau, T. J. and Macfarlane, A. H.: Reduced growth rate of *Montastrea annularis* following the  
26 1987–1988 coralbleaching event, Coral Reefs, 8, 211-215, 1990.

27 Gothmann, A. M., Stolarski, J., Adkins, J. F., Schoene, B., Dennis, K. J., Schrag, D. P., Mazur, M.,  
28 and Bender, M. L.: Fossil corals as an archive of secular variations in seawater chemistry since the  
29 Mesozoic, Geochimica et Cosmochimica Acta, 160, 188-208, 2015.

30 Graus, R. R. and Macintyre, I. G.: Variations in growth forms of the reef coral *Montastrea annularis*  
31 (Ellis & Sollander): a quantitative evaluation of growth response to light distribution using computer  
32 simulation. In: The Atlantic Barrier Reef Ecosystem at Carrie Bow Cay, Belize, I — Structure and  
33 Communities, Rützler, K. and Macintyre, I. G. (Eds.), Smithsonian Contributions to the Marine  
34 Sciences No. 12, Washington, D.C., 1982.

35 Griffiths, N., Müller, W., Johnson, K. G., and Aguilera, O. A.: Evaluation of the effect of diagenetic  
36 cements on element/Ca ratios in aragonitic Early Miocene (~16 Ma) Caribbean corals: Implications for  
37 "deep-time" palaeoenvironmental reconstructions, Palaeogeography Palaeoclimatology Palaeoecology,  
38 369, 185-200, 2013.

39 Grizzle, R. E., Bricelj, V. M., and Shumway, S. E.: Physiological ecology of *Mercenaria mercenaria*.  
40 In: The biology of the hard clam, Kraeuter, J. N. and Castagna, M. (Eds.), Developments in  
41 aquaculture and fisheries science, 31, Elsevier, Amsterdam, 2001.

42 Hallock, P. and Schlager, W.: Nutrient excess and the demise of coral reefs and carbonate platforms,  
43 Palaios, 1, 389-398, 1986.

44 Helmle, K. P., Dodge, R. E., Swart, P. K., Gledhill, D. K., and Eakin, C. M.: Growth rates of Florida  
45 corals from 1937 to 1996 and their response to climate change, Nature Communications, 2, 6, 2011.

46 Helmle, K. P., Kohler, K. E., and Dodge, R. E.: The coral X-radiograph densitometry system:  
47 CoralXDS. Nova Southeastern University, Fort-Lauderdale-Davie, 2002.

48 Highsmith, R. C.: Coral growth rates and environmental control of density banding, Journal of  
49 Experimental Marine Biology and Ecology, 37, 105-125, 1979.

50 Highsmith, R. C., Lueptow, R. L., and Schonberg, S. C.: Growth and bioerosion of three massive  
51 corals on the Belize barrier reef, Marine Ecology Progress Series, 13, 261-271, 1983.

52 Hofmann, G. E., Smith, J. E., Johnson, K. S., Send, U., Levin, L. A., Micheli, F., Paytan, A., Price, N.  
53 N., Peterson, B., Takeshita, Y., Matson, P. G., Derse Crook, E., Kroeker, K. J., Gambi, M. C., Rivest,  
54 E. B., Frieder, C. A., Yu, P. C., and Martz, T. R.: High-Frequency Dynamics of Ocean pH: A Multi-  
55 Ecosystem Comparison, PLoS ONE, 6, 2011.

1 Hönisch, B., Ridgwell, A., Schmidt, D. N., Thomas, E., Gibbs, S. J., Slujis, A., Zeebe, R., Kump, L.,  
2 Martindale, R. C., Greene, S. E., Kiessling, W., Ries, J., Zachos, J. C., Royer, D. L., Barker, S.,  
3 Marchitto, T. M., Moyer, R., Pelejero, C., Ziveri, P., Foster, G. L., and Williams, B.: The geological  
4 record of ocean acidification, *Science*, 335, 1058-1063, 2012.

5 Hudson, J. H., Powell, G. V. N., Robblee, M. B., and Smith, T. J., III: A 107-year-old coral from  
6 Florida Bay: barometer of natural and man-induced catastrophies?, *Bulletin of Marine Science*, 44,  
7 283-291, 1989.

8 IPCC: Summary for Policymakers. In: *Climate Change 2013: The Physical Science Basis. Contribution of Working Group I to the Fifth Assessment Report of the Intergovernmental Panel on*  
9 *Climate Change*, Stocker, T., Qin, D., Plattner, G.-K., Tignor, M. M. B., Allen, S. K., Boschung, J.,  
10 Nauels, A., Xia, Y., Bex, V., and Midgley, P. M. (Eds.), Cambridge University Press, Cambridge,  
11 United Kingdom and New York, NY, USA, 2013.

12 Jochum, K. P., Weis, U., Stoll, B., Kuzmin, D., Yang, Q., Raczek, I., Jacob, D. E., Stracke, A.,  
13 Birbaum, K., Frick, D. A., Günther, D., and Enzweiler, J.: Determination of reference values for NIST  
14 SRM 610-617 glasses following ISO guidelines, *Geostandards and Geoanalytical Research*, 35, 397-  
15 429, 2011.

16 Johnson, K. G. and Pérez, M. E.: Skeletal extension rates of Cenozoic Caribbean reef corals, *Palaios*,  
17 21, 262-271, 2006.

18 Jones, D. S. and Allmon, W. D.: Records of upwelling, seasonality and growth in stable-isotope  
19 profiles of Pliocene mollusk shells from Florida, *Lethaia*, 28, 61-74, 1995.

20 Kiessling, W., Simpson, C., Beck, B., Mewis, H., and Pandolfi, J. M.: Equatorial decline of reef corals  
21 during the last Pleistocene interglacial, *Proceedings of the National Academy of Sciences*, 109, 21378-  
22 21383, 2012.

23 Klein, R., Pätzold, J., Wefer, G., and Loya, Y.: Depth-related timing of density band formation in  
24 *Porites* spp. corals from the Red Sea inferred from X-ray chronology and stable isotope composition,  
25 *Marine Ecology Progress Series*, 97, 99-104, 1993.

26 Knutson, D. W., Buddemeier, R. W., and Smith, S. V.: Coral chronometers: seasonal growth bands in  
27 reef corals, *Science*, 177, 270-272, 1972.

28 Kuffner, I. B., Hickey, T. D., and Morrison, J. M.: Calcification rate of the massive coral *Siderastrea*  
29 *sidera* and crustose coralline algae along the Florida Keys (USA) outer-reef tract, *Coral Reefs*, 32,  
30 987-997, 2013.

31 Langdon, C., Takahashi, T., Sweeney, C., Chipman, D., and Goddard, J.: Effect of calcium carbonate  
32 saturation on the calcification rate of an experimental coral reef, *Global Biogeochemical Cycles*, 14,  
33 639-654, 2000.

34 Leder, J. J., Swart, P. K., Szmant, A., and Dodge, R. E.: The origin of variations in the isotopic record  
35 of scleractinian corals: 1. Oxygen, *Geochimica et Cosmochimica Acta*, 60, 2857-2870, 1996.

36 Lidz, B. H.: Florida Keys. In: *Encyclopedia of modern coral reefs - structure, form and process*,  
37 Hopley, D. (Ed.), Springer, Dordrecht, 2011.

38 Lloyd, R. M.: A palaeoecological interpretation of the Caloosahatchee Formation, using stable isotope  
39 methods, *Journal of Geology*, 77, 1-25, 1969.

40 Lough, J. M.: Coral calcification from skeletal records revisited, *Marine Ecology Progress Series*, 373,  
41 257-264, 2008.

42 Lough, J. M. and Barnes, D. J.: Environmental controls on growth of the massive coral *Porites*,  
43 *Journal of Experimental Marine Biology and Ecology*, 245, 225-243, 2000.

44 Lough, J. M. and Cooper, T. F.: New insights from coral growth band studies in an era of rapid  
45 environmental change, *Earth-Science Reviews*, 108, 170-184, 2011.

46 Macintyre, I. G. and Pilkey, O. H.: Tropical Reef Corals: Tolerance of Low Temperatures on the  
47 North Carolina shelf, *Science*, 166, 374-375, 1969.

48 Mallela, J. and Perry, C. T.: Calcium carbonate budgets for two coral reefs affected by different  
49 terrestrial runoff regimes, Rio Bueno, Jamaica, *Coral Reefs*, 26, 129-145, 2007.

50 Manzello, D. P., Enochs, I. C., Bruckner, A., Renaud, P. G., Kolodziej, G., Budd, D. A., Carlton, R.,  
51 and Glynn, P. W.: Galapagos coral reef persistence after ENSO warming across an acidification  
52 gradient, *Geophys. Res. Lett.*, 41, 9001-9008, 2014.

53 Manzello, D. P., Enochs, I. C., Kolodziej, G., and Carlton, R.: Coral growth patterns of *Montastraea*  
54 *cavernosa* and *Porites astreoides* in the Florida Keys: The importance of thermal stress and inimical  
55 waters, *Journal of Experimental Marine Biology and Ecology*, 471, 198-207, 2015a.

1 Manzello, D. P., Enochs, I. C., Kolodziej, G., and Carlton, R.: Recent decade of growth and  
2 calcification of *Orbicella falveolata* in the Florida Keys: an inshore-offshore comparison, *Marine*  
3 *Eology Progress Series*, 521, 81-89, 2015b.

4 McCulloch, M., Fallon, S., Wyndham, T., Hendy, E., Lough, J., and Barnes, D.: Coral record of  
5 increased sediment flux to the inner Great Barrier Reef since European settlement, *Nature*, 421, 727-  
6 730, 2003.

7 McGregor, H. V. and Gagan, M. K.: Diagenesis and geochemistry of *Porites* corals from Papua New  
8 Guinea: Implications for paleoclimate reconstruction, *Geochimica et Cosmochimica Acta*, 67, 2147-  
9 2156, 2003.

10 Meeder, J. F.: A field guide with road log to "The Pliocene fossil reef of southwest Florida", Miami,  
11 19, 1979.

12 Mertz-Kraus, R.: Mediterranean-type climate in the south Aegean (Eastern Mediterranean) during the  
13 Late Miocene: Evidence from isotope and element proxies, Dr. rer. nat. Dissertation, Fachbereich  
14 Chemie, Pharmazie und Geowissenschaften, Universität Mainz, Mainz, 129 pp., 2009.

15 Mertz-Kraus, R., Brachert, T. C., Jochum, K. P., Reuter, M., and Stoll, B.: LA-ICP-MS analyses on  
16 coral growth increments reveal heavy winter rain in the Eastern Mediterranean at 9 Ma,  
17 *Palaeogeography, Palaeoclimatology, Palaeoecology*, 273, 25-40, 2009a.

18 Mertz-Kraus, R., Brachert, T. C., and Reuter, M.: *Tarbellastraea* (Scleractinia): A new stable isotope  
19 archive for Late Miocene paleoenvironments in the Mediterranean, *Palaeogeography,*  
20 *Palaeoclimatology, Palaeoecology*, 257, 294-307, 2008.

21 Mertz-Kraus, R., Brachert, T. C., Reuter, M., Galer, S. J. G., Fassoulas, C., and Iliopoulos, G.: Late  
22 Miocene sea surface salinity variability in the Eastern Mediterranean inferred from coral aragonite  
23  $\delta^{18}\text{O}$  (Crete, Greece), *Chemical Geology*, 262, 202-216, 2009b.

24 Miller, K. G., Wright, J. D., Browning, J. V., Kulpecz, A., Kominz, M., Naish, T. R., Cramer, B. S.,  
25 Rosenthal, Y., Peltier, W. R., and Sostdian, S.: High tide of the warm Pliocene: Implications of global  
26 sea level for Antarctic deglaciation, *Geology*, doi: doi:10.1130/G32869.1, 2012. 1-4, 2012.

27 Nothdurft, L. D. and Webb, G. E.: Earliest diagenesis in scleractinian coral skeletons: implications for  
28 palaeoclimate-sensitive geochemical archives, *Facies*, 55, 161-201, 2009.

29 O'Brien, C. L., Foster, G. L., Martinez-Boti, M. A., Abell, R., Rae, J. W. B., and Pancost, R. D.: High  
30 sea surface temperatures in tropical warm pools during the Pliocene, *Nature Geoscience*, 7, 606-611,  
31 2014.

32 Okazaki, R. R., Swart, P. K., and Langdon, C.: Stress-tolerant corals of Florida Bay are vulnerable to  
33 ocean acidification, *Coral Reefs*, doi: 10.1007/s00338-013-1015-3, 2013. 2013.

34 Perrin, C.: Diagenèse précoce des biocristaux carbonatés : transformations isominérales de l'aragonite  
35 corallienne, *Bulletin de la Société Géologique de France*, 175, 95-106, 2004.

36 Petit, J. R., Jouzel, J., Raynaud, D., Barkov, N. I., Barnola, J.-M., Basile, I., Bender, M., Chappellaz,  
37 J., Davis, M., Delaygue, G., Delmotte, M., Kotlyakov, V. M., Legrand, M., Lipenkov, V. Y., Lorius,  
38 C., Pépin, L., Ritz, C., Saltzman, E., and Stievenard, M.: Climate and atmospheric history of the past  
39 420,000 years from the Vostok ice core, Antarctica, *Nature*, 399, 429-436, 1999.

40 Petuch, E. J. and Roberts, C. E.: *The geology of the Everglades and adjacent areas*, CRC Press, New  
41 York and Boca Raton, 2007.

42 Reuter, M., Brachert, T. C., and Kroeger, K. F.: Diagenesis of growth bands in fossil scleractinian  
43 corals: Identification and modes of preservation, *Facies*, 51, 155-168, 2005.

44 Riding, R., Liang, L., and Braga, J.-C.: Millennial-scale ocean acidification and late Quaternary  
45 decline of cryptic bacterial crusts in tropical reefs, *Geobiology*, doi: 10.1111/gbi.12097, 2014. 1-19,  
46 2014.

47 Riegl, B. and Piller, W. E.: Possible refugia for reefs in times of environmental stress, *International*  
48 *Journal of Earth Sciences*, 92, 520-531, 2003.

49 Roulier, L. M. and Quinn, T. M.: Seasonal- to decadal-scale climatic variability in southwest Florida  
50 during the middle Pliocene: Inferences from a coralline stable isotope record, *Paleoceanography*, 10,  
51 429-443, 1995.

52 Schroeder, J. H. and Purser, B. H. (Eds.): *Reef Diagenesis*, Springer-Verlag, New York, 1986.

53 Seki, O., Foster, G. L., Schmidt, D. N., Mackensen, A., Kawamura, K., and Pancost, R. D.: Alkenone  
54 and boron-based Pliocene  $p\text{CO}_2$  records, *Earth and Planetary Science Letters*, 292, 201-211, 2010.

55 Shen, G. T. and Dunbar, R. B.: Environmental controls on uranium in reef corals, *Geochimica et*  
56 *Cosmochimica Acta*, 59, 2009-2024, 1995.

1 Shinn, E. A.: Coral growth-rate, an environmental indicator, *Journal of Paleontology*, 40, 233-240,  
2 1966.

3 Sinclair, D. J., Kinsley, L. P. J., and McCulloch, M. T.: High resolution analysis of trace elements in  
4 corals by laser ablation ICP-MS, *Geochimica et Cosmochimica Acta*, 62, 1889-1901, 1998.

5 Swart, P. K.: Carbon and oxygen isotope fractionation in scleractinian corals: A review, *Earth-Science*  
6 *Reviews*, 19, 51-80, 1983.

7 Swart, P. K.: The strontium, magnesium and sodium composition of recent scleractinian coral  
8 skeletons as standards for palaeoenvironmental analysis, *Palaeogeography, Palaeoclimatology,*  
9 *Palaeoecology*, 34, 115-136, 1981.

10 Swart, P. K., Greer, L., Rosenheim, B. E., Moses, C. S., Waite, A. J., Winter, A., Dodge, R. E., and  
11 Helmle, K.: The  $^{13}\text{C}$  Suess effect in scleractinian corals mirror changes in the anthropogenic  $\text{CO}_2$   
12 inventory of the surface oceans, *Geophysical Research Letters*, 37, L05604, 2010.

13 Swart, P. K., Healy, G., Greer, L., Lutz, M., Saied, A., Anderegg, D., Dodge, R. E., and Rudnick, D.:  
14 The use of proxy chemical records in coral skeletons to ascertain past environmental conditions in  
15 Florida Bay, *Estuaries*, 22, 384-397, 1999.

16 Swart, P. K., Healy, G. F., Dodge, R. E., Kramer, P., Hudson, J. H., Halley, R. B., and Robblee, M. B.:  
17 The stable oxygen and carbon isotopic record from a coral growing in Florida Bay: a 160 year record  
18 of climatic and anthropogenic influence, *Palaeogeography, Palaeoclimatology, Palaeoecology*, 123,  
19 219-237, 1996.

20 Tanzil, J. T. I., Brown, B. E., Tudhope, A. W., and Dunne, R. P.: Decline in skeletal growth of the  
21 coral *Porites lutea* from the Andaman Sea, South Thailand between 1984 and 2005, *Coral Reefs*, doi:  
22 10.1007/s00338-008-0457-5, 2009. 2009.

23 Tao, K. and Grossman, E. L.: Origin of high productivity in the Pliocene of the Florida platform:  
24 Evidence from stable isotopes, *Palaios*, 25, 796-806, 2010.

25 Townsend, C. R., Begon, M., and Harper, J. L.: *Essentials of Ecology*, Blackwell, Oxford, 2008.

26 Worum, F. P., Carricart-Ganivet, J. P., Besnon, L., and Golicher, D.: Simulation and observation of  
27 annual density banding in skeletons of *Montastrea* (Cnidaria: Scleractinia) growing under thermal  
28 stress associated with ocean warming, *Limnology and Oceanography*, 52, 2317-2323, 2007.

29

30

1 Table 1. Sampling sites in southern Florida. The numbering follows that given by Brachert et  
 2 al. (2014).

<u>No.</u>	<u>Site</u>	<u>Sample ID</u>	<u>Genus</u>	<u>GPS Coordinates</u>	<u>Lithostratigraphy</u>	<u>Age (Ma)</u>
4	Palm Beach Aggregates	EP8 EP9A EP9B EP9C EP9D	<i>Solenastrea</i> <i>Solenastrea</i> <i>Orbicella</i> <i>Solenastrea</i> <i>Solenastrea</i>	26°41.742'N, 80°21.270'W	Bermont Fm. (Holey Land Mb.)	1.2
8	Brantley Pit, Arcadia	EP6-S2	<i>Solenastrea</i>	27°2.988'N, 81°49.611'W	Caloosahatchee Fm. (Bee Branch Mb.)	1.8
9	DeSoto Sand and Shell LLC (site 452)	452-K1-S6* 452-K3* 452-K4 452-K5* 452-13* 452-K14 452-K15* 452-K17*	<i>Solenastrea</i> <i>Solenastrea</i> <i>Solenastrea</i> <i>Solenastrea</i> <i>Solenastrea</i> <i>Solenastrea</i> <i>Solenastrea</i> <i>Solenastrea</i>	27°3.587'N, 81°47.627'W	Caloosahatchee Fm. (Bee Branch Mb.)	1.8
15	Mule Pen Quarry	EP1-S2 EP2-S2 EP3 EP5-S2	<i>Solenastrea</i> <i>Orbicella</i> <i>Porites</i> <i>Solenastrea</i>	26°10.410'N, 81°42.468'W	Tamiami Fm. (Golden Gate Mb.)	2.9
16	Quality Aggregates (APAC)	Coral #1**	<i>Solenastrea</i>	Not available.	Tamiami Fm. (Pinecrest Mb., unit 7)	3.2

3 \* from Böcker (2014)

4 \*\* from Roulier & Quinn (1995)

5

6

1 Table 2. Extension rate, bulk density and calcification rate in recent and fossil reef corals.

2 **Bold: minimum values.**

<u>Taxon</u>	<u>n</u>	<u>Minimum</u> <u>mean</u> <u>extension</u> <u>rate (cm</u> <u>yr<sup>-1</sup>)</u>	<u>Maximum</u> <u>mean</u> <u>extension</u> <u>rate (cm</u> <u>yr<sup>-1</sup>)</u>	<u>Mean</u> <u>extension</u> <u>rate (cm</u> <u>yr<sup>-1</sup>)</u>	<u>Minimum</u> <u>bulk</u> <u>density (g</u> <u>cm<sup>-3</sup>)</u>	<u>Maximum</u> <u>bulk</u> <u>density (g</u> <u>cm<sup>-3</sup>)</u>	<u>Mean</u> <u>bulk</u> <u>density</u> <u>(g cm<sup>-3</sup>)</u>	<u>Minimum</u> <u>calcification</u> <u>rate (g cm<sup>-2</sup></u> <u>yr<sup>-1</sup>)</u>	<u>Maximum</u> <u>calcification</u> <u>rate (g cm<sup>-2</sup></u> <u>yr<sup>-1</sup>)</u>	<u>Mean</u> <u>calcification</u> <u>rate (g cm<sup>-2</sup></u> <u>yr<sup>-1</sup>)</u>
<i>Orbicella</i>	80	0.38	1.44	0.91 ± 0.23	0.78	1.94	1.37 ± 0.24	0.65	1.78	1.22 ± 0.25
<i>Diploria</i>	8	0.30	<b>0.40</b>	<b>0.35</b> ± 0.04	0.97	1.70	1.27 ± 0.31	0.31	0.68	0.45 ± 0.14
<i>Porites</i> (W- Atlantic)	15	0.28	0.48	0.37 ± 0.07	1.10	1.72	1.44 ± 0.20	0.31	0.77	0.53 ± 0.14
<i>Porites</i> (Indo- Pacific)	78	0.30	2.38	1.28 ± 0.50	1.01	1.90	1.30 ± 0.16	0.56	2.82	1.67 ± 0.49
<i>Solenastrea</i> (Florida Bay, recent);	1			0.54			1.07			0.57
<i>Solenastrea</i> (1.2, 1.8, 2.9, 3.2 Ma)	12	0.22	0.83	0.42 ± 0.17	<b>0.55</b>	1.22	0.87 ± 0.22	0.20	0.97	0.38
<i>Orbicella</i> (1.2, 2.9 Ma)	2	<b>0.16</b>	0.64	0.40	0.76	<b>1.14</b>	0.95	<b>0.18</b>	<b>0.48</b>	<b>0.33</b>
<i>Porites</i> (2.9 Ma)	1			0.89			<b>0.60</b>			0.54

3

4

1 Table 3: Bulk calcification data of recent reef corals in the Indo-Pacific and Western Atlantic  
 2 together with fossil reef corals from Florida (USA). Bold: minimum values.

<u>Region with geological age</u>	<u>n</u>	<u>Extension min (cm yr<sup>-1</sup>)</u>	<u>Extension max (cm yr<sup>-1</sup>)</u>	<u>Extension mean (cm yr<sup>-1</sup>)</u>	<u>Density min (g cm<sup>-3</sup>)</u>	<u>Density max (g cm<sup>-3</sup>)</u>	<u>Density mean (g cm<sup>-3</sup>)</u>	<u>Calc min (g cm<sup>-2</sup> yr<sup>-1</sup>)</u>	<u>Calc max (g cm<sup>-2</sup> yr<sup>-1</sup>)</u>	<u>Calc mean (g cm<sup>-2</sup> yr<sup>-1</sup>)</u>
Indo-Pacific, recent	78	0.30	2.38	1.28 ± 0.50	1.01	1.90	1.30 ± 0.16	0.56	2.82	1.67 ± 0.49
Western Atlantic, recent	103	0.28	1.44	0.79 ± 0.31	0.78	1.94	1.37 ± 0.24	0.31	1.78	1.06 ± 0.38
Florida Bay, recent	1			0.54			1.07			0.57
Florida (USA), Plio-Pleistocene	15	<b>0.16</b>	<b>0.86</b>	<b>0.44</b> ± 0.19	<b>0.55</b>	<b>1.22</b>	<b>0.86</b> ± 0.22	<b>0.18</b>	<b>0.54</b>	<b>0.34</b> ± 0.11

3

4

1 Table 4. Calcification data from recent z-corals, southern Florida

Taxon and site	Extension rate	Bulk density	Calcification rate	Source
<i>Solenastrea</i> , Florida Bay	0.89	N.A.	N.A.	(Hudson et al., 1989)
<i>Solenastrea</i> , FB (FB-6)	0.51	N.A.	N.A.	(Swart et al., 1996)
<i>Porites</i> , FRT, inshore	0.43	1.61	0.69	(Manzello et al., 2015a)
<i>Porites</i> , FRT, offshore	0.35	1.58	0.55	(Manzello et al., 2015a)
<i>Orbicella</i> , FRT	0.79	1.18	0.91	(Helmle et al., 2011)
<i>Solenastrea</i> , FB (FB-6)	0.54	1.07	0.58	this work

2

3



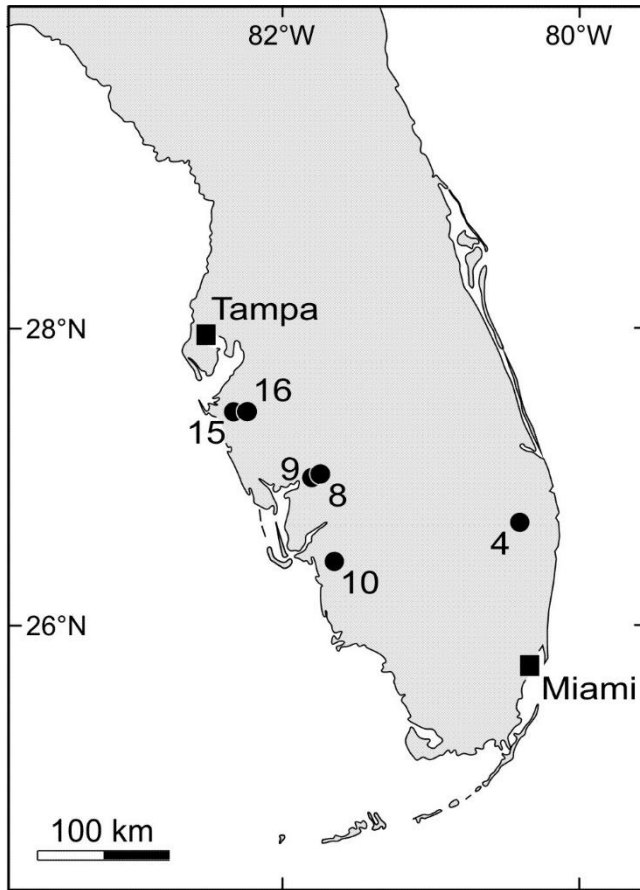


# Figure 1

1

2 Figure 1. Sampling stations in southern Florida/USA (dots). See Table 1 for details and  
3 numbering of sampling stations.

4

5

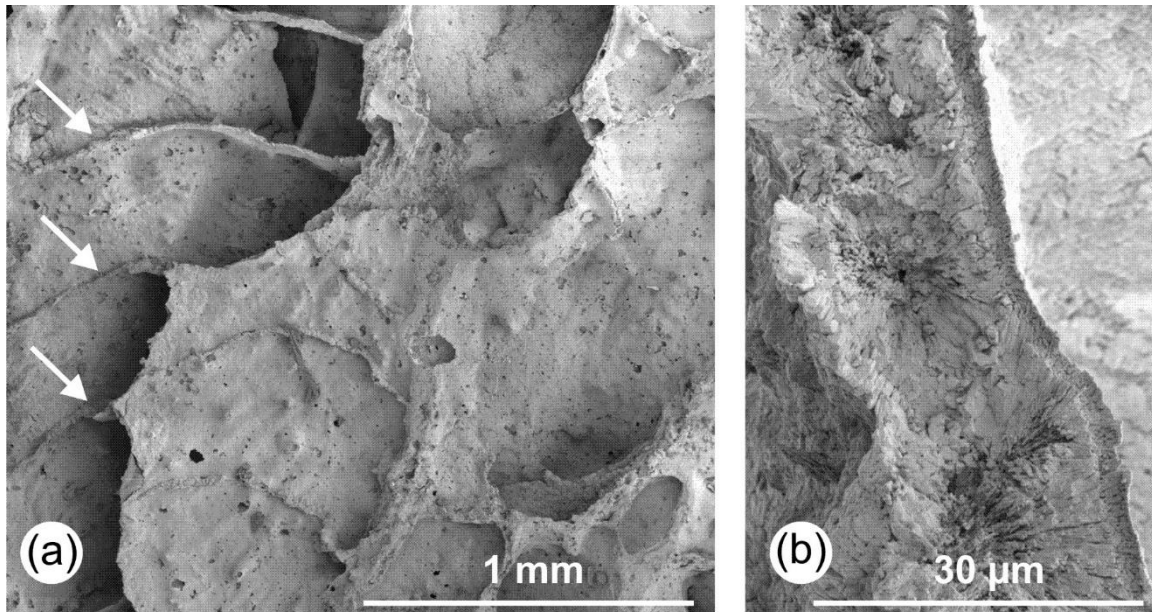


## Figure 2

1  
2  
3  
4  
5  
6  
7  
8  
9

Figure 2. SEM images of fossil coral skeleton (*Solenastrea* sp. EP 6), Caloosahatchee Fm. (1.8 Ma), Brantley Pit, Florida/USA. A: Overview of septal surfaces. Curved ridges represent the traces of broken dissepiments (arrows). Holes within septa are mechanical defects. B: Cross-section of dissepiment showing radial fiber architecture of sclerodermites. Note minor preferential dissolution at the centers of the trabecular fans.

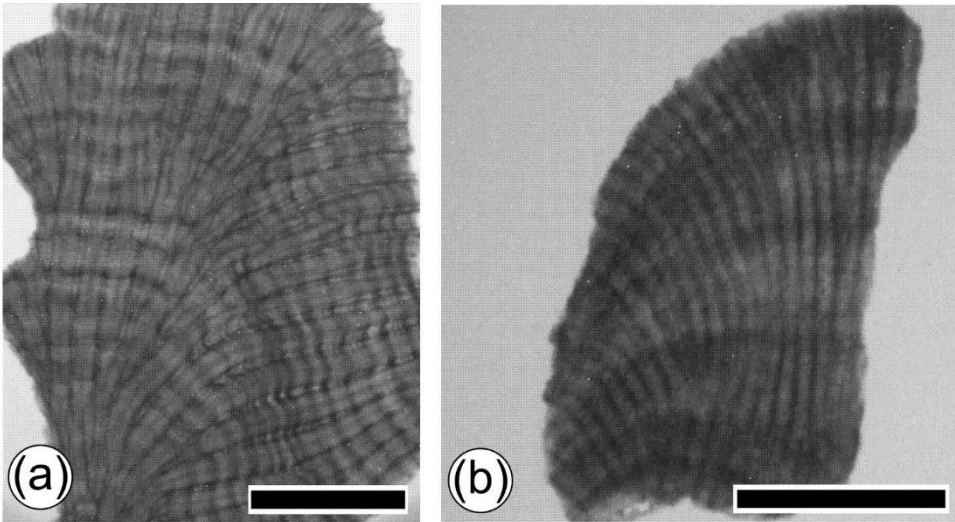


### Figure 3

1  
2  
3  
4  
5  
6  
7

Figure 3. Digital X-ray photographs (positive prints) from fossil z-corals. A: *Solenastrea* sp. (EP 5, Mule Pen Quarry, Tamiami Fm., age 2.5 Ma). B: *Porites* sp. (EP3, Mule Pen Quarry, Tamiami Fm., age 2.9 Ma). Scale bar 2 cm.

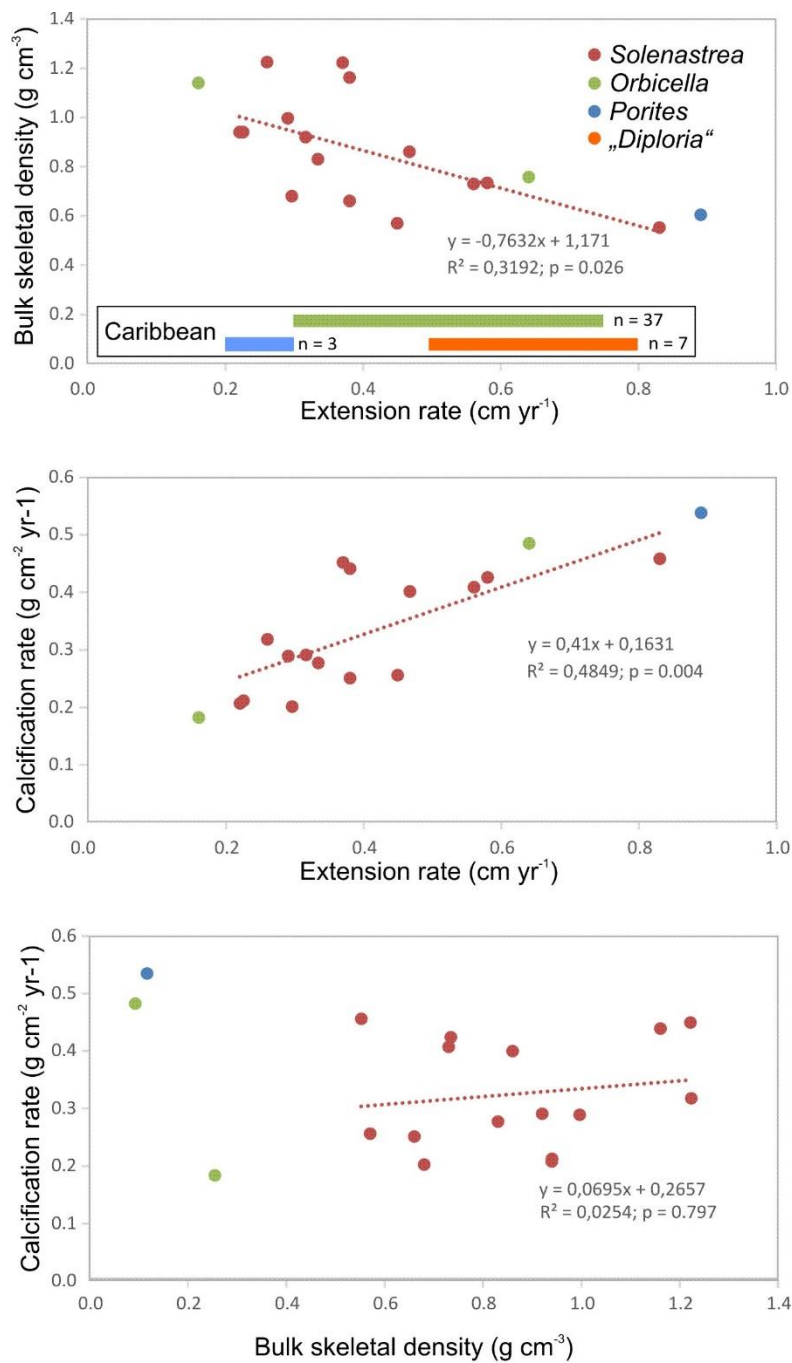


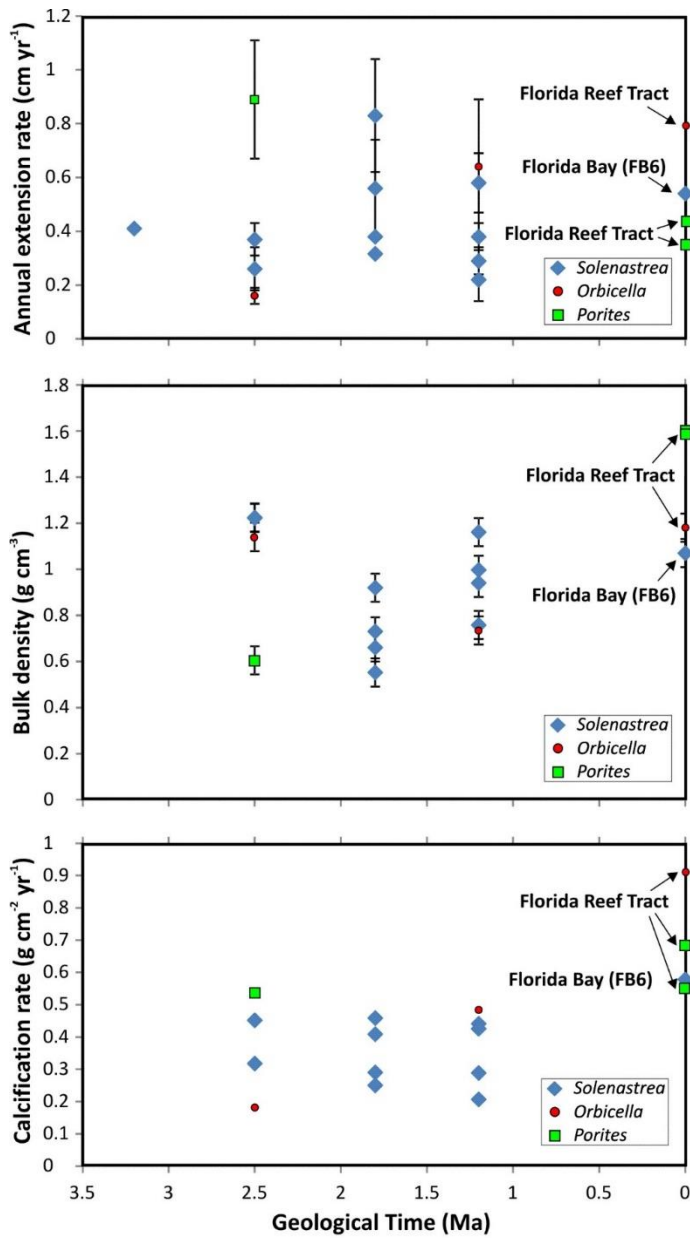
## Figure 4

- 1
- 2 Fig. 4. Calcification systematics in three Pliocene and Pleistocene z-coral genera from the
- 3 Florida Platform. Inset summarizes published extension rates from the Pliocene of the
- 4 Caribbean region; corresponding density values and calcification rates are not available
- 5 (Johnson and Pérez, 2006). “*Diploria*” refers to the two taxa *Diploria* and *Pseudodiploria*
- 6 (Budd et al., 2012).

7



1



2

## Figure 5

3

Figure 5. Temporal variation of the mean extension rate ( $\pm 1\sigma$ ), bulk density and mean

4

calcification rate in three *z*-coral genera (*Solenastrea*, *Orbicella*, *Porites*) from the Pliocene -

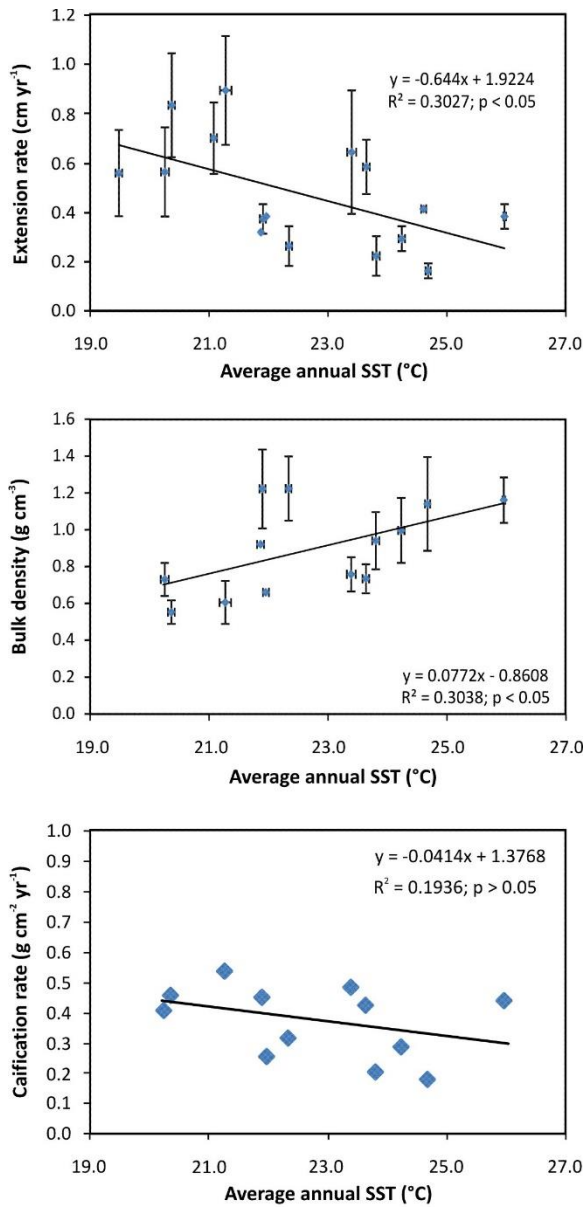
5

Pleistocene Florida platform. Recent data from (Helmle et al., 2011; Hudson et al., 1989;

6

Manzello et al., 2015a; Swart et al., 1996) and own materials (Florida Bay).

7

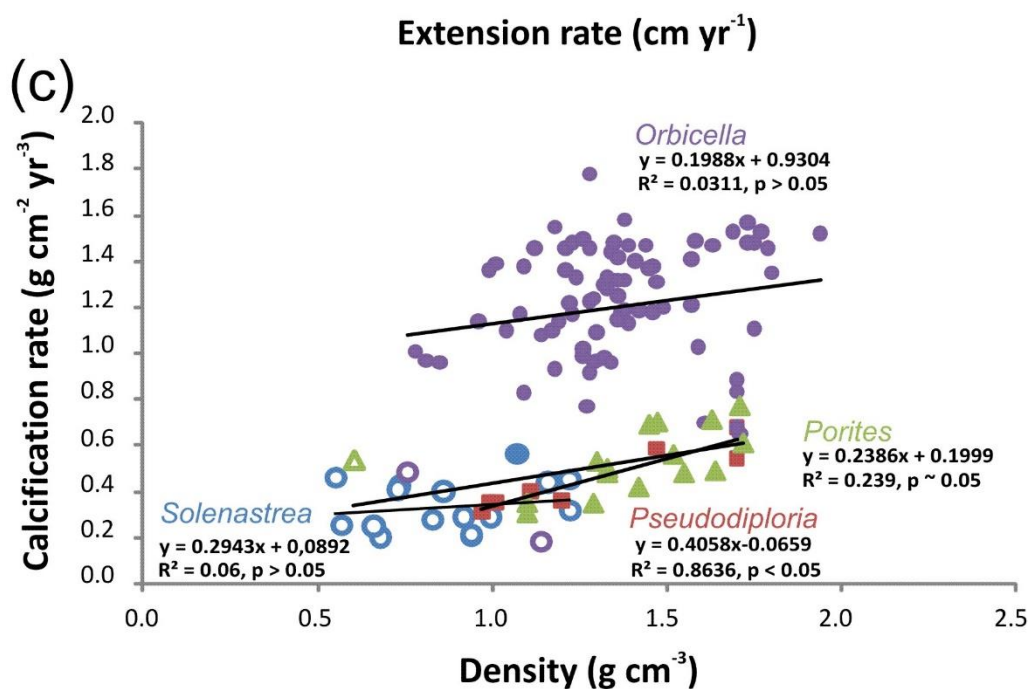
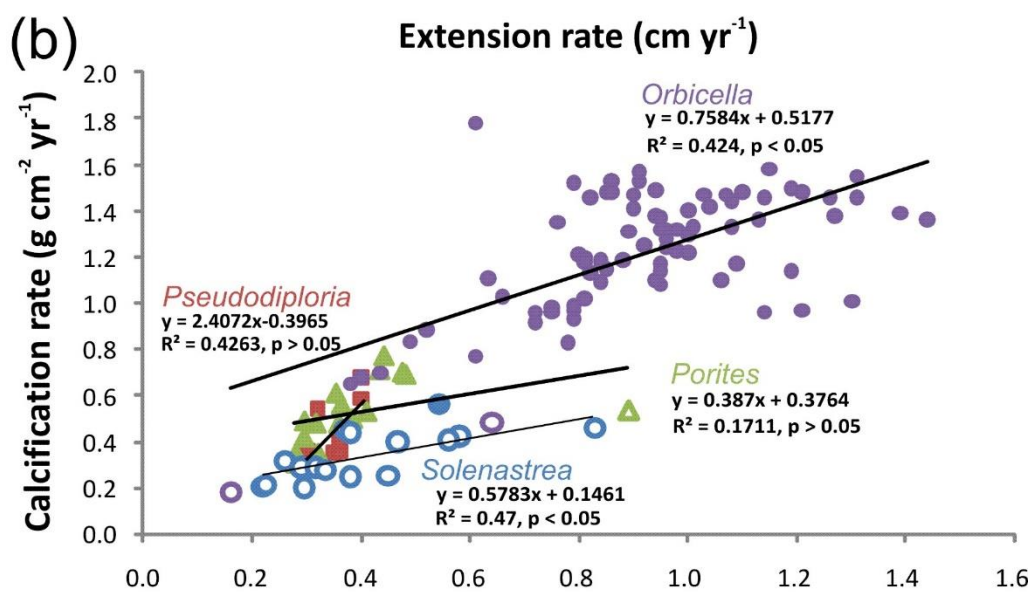
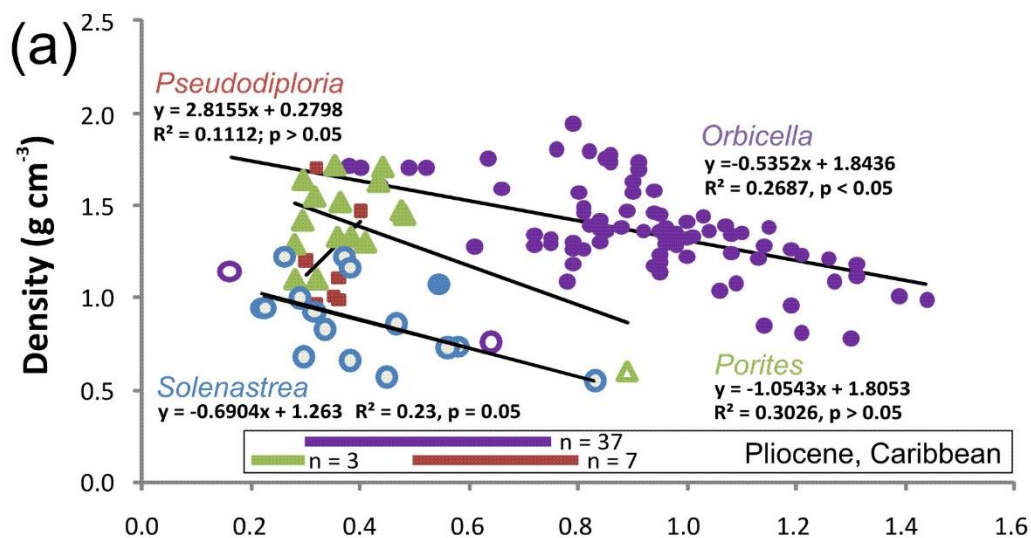


## 1 Figure 6

2 Figure 6. Diagrams showing annual extension rate (cm yr<sup>-1</sup>), bulk density (g cm<sup>-3</sup>) and annual  
 3 calcification rate (g cm<sup>-2</sup> yr<sup>-1</sup>) with water temperature inferred from published  $\delta^{18}\text{O}$  values  
 4 (Brachert et al., 2014).

5

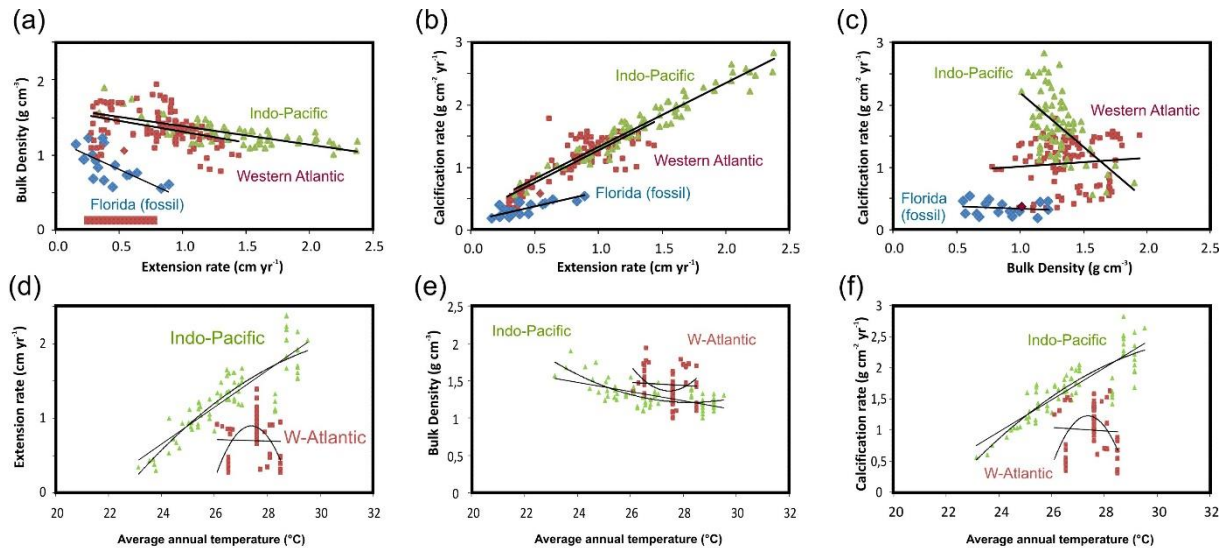
6



1 Figure 7



1 Figure 7. Mean extension rate, bulk skeletal density and mean calcification rate of reef corals  
2 sorted according to taxon and geological time (Western Atlantic region). Magenta: *Orbicella*,  
3 green: *Porites*, red: *Diploria*, blue: *Solenastrea*. Filled symbols: recent, open symbols: fossil.  
4 Data on recent corals compiled from the literature (Carricart-Ganivet et al., 2000; Carricart-  
5 Ganivet and Merino, 2001; Dodge and Brass, 1984; Elizalde-Rendon et al., 2010; Highsmith  
6 et al., 1983; Hudson et al., 1989; Mallela and Perry, 2007) and one unpublished record from  
7 *Solenastrea* (FB-6). Inset in uppermost panel shows range of extension rates of z-corals of  
8 Pliocene age in the Caribbean region (various taxa) for comparison (Johnson and Pérez,  
9 2006). Note clustering of fossil corals at low extension rates, low density and low  
10 calcification rates.  
11



1 **Figure 8**

2 Figure 8. Experimental data of extension rate, density and calcification rate of recent and  
 3 fossil z-corals. Indo-Pacific (green triangles), Western Atlantic (red squares) and Florida  
 4 fossils (blue diamonds). A – C: Descriptive diagrams for relationships of extension rate,  
 5 density, and calcification rate within the temperature windows shown in D – F for modern  
 6 corals. Recent corals compiled from literature (Carricart-Ganivet et al., 2000; Carricart-  
 7 Ganivet and Merino, 2001; Dodge and Brass, 1984; Elizalde-Rendon et al., 2010; Highsmith  
 8 et al., 1983; Hudson et al., 1989; Lough, 2008; Mallela and Perry, 2007; Tanzil et al., 2009).  
 9 Red horizontal bar in figure 7A summarizes published extension rates of z-corals of Pliocene  
 10 age in the Caribbean region (various taxa) for comparison (Johnson and Pérez, 2006). D – F:  
 11 Extension rate, bulk density and calcification rates as a function of average annual  
 12 temperature. Results of linear and quadratic polynomial regression are as follows: **(a)** Western  
 13 Atlantic  $y = -0.2958x + 1,6072$ ;  $R^2 = 0.1399$ ,  $p < 0.05$ . Indo-Pacific  $y = -0.2499x + 1.6358$ ;  $R^2$   
 14  $= 0.5167$ ,  $p < 0.05$ . Florida (fossils)  $y = -0.7607x + 1.2774$ ;  $R^2 = 0.4297$ ,  $p < 0.05$ . **(b)** Western  
 15 Atlantic  $y = 1.0235x + 0.2545$ ;  $R^2 = 0.6956$ ,  $p < 0.05$ . Indo-Pacific  $y = 1.0212x + 0.3064$ ;  $R^2$   
 16  $= 0.9327$ ,  $p < 0.05$ . Florida (fossils)  $y = 0.4961x + 0.1648$ ;  $R^2 = 0.3171$ ,  $p < 0.05$ . **(c)** Western  
 17 Atlantic  $y = 0.1428x + 0.868$ ;  $R^2 = 0.0084$ ,  $p > 0.05$ . Indo-Pacific  $y = -1.7219x + 3.9122$ ;  $R^2$   
 18  $= 0,3204$ ,  $p < 0.05$ . Florida (fossils)  $y = -0.0779x + 0.4058$ ;  $R^2 = 0.0233$ ,  $p > 0.05$ . **(d)** Western  
 19 Atlantic  $y = -0.3747x^2 + 20.525x - 280.21$ ;  $R^2 = 0.3524$ ;  $p < 0.05$  and  $y = -0.0104x + 0.9913$ ;  $R^2$   
 20  $= 0.0006$ ;  $p > 0.05$ . Indo-Pacific  $y = -0.0203x^2 + 3.294x - 19.628$ ;  $R^2 = 0.7519$ ;  $p < 0.05$  and  $y$   
 21  $= 0.2472x - 5.282$ ;  $R^2 = 0.7376$ ;  $p < 0.05$ . **(e)** Western Atlantic  $y = 0.1588x^2 - 8,7235x + 121.16$ ;  
 22  $R^2 = 0.1128$ ;  $p > 0.05$  and  $y = -0.0193x + 1.9758$ ;  $R^2 = 0.0036$ ;  $p > 0.05$ . Indo-Pacific  $y = 0.0206x^2 -$   
 23  $1.1664x + 17.691$ ;  $R^2 = 0.5101$ ;  $p < 0.05$  and  $y = -0.0613x + 2.9539$ ;  $R^2 = 0.3885$ ;  $p < 0.05$ . **(f)**  
 24 Western Atlantic  $y = -0.4333x^2 + 23.722x - 323.44$ ;  $R^2 = 0.2699$ ;  $p < 0.05$  and  $y = -$   
 25  $0.0282x + 1.7778$ ;  $R^2 = 0.0025$ ;  $p > 0.05$ . Indo-Pacific  $y = -0.0223x^2 + 1.4534x - 21.144$ ;  $R^2$   
 26  $= 0.7476$ ;  $p < 0.05$  and  $y = 0.2566x - 5.1844$ ;  $R^2 = 0.7322$ ;  $p < 0.05$ .

